UNIVERSIDADE DA BEIRA INTERIOR
Engenharia

Design of a Supersonic Nozzle

João Pedro Ramalho Lopes

Dissertação para obtenção do Grau de Mestre em
Engenharia Aeronáutica
(ciclo de estudos integrado)

Orientador: Prof. Doutor Francisco Miguel Ribeiro Proença Brojo

Covilhã, Fevereiro de 2020

Dedicatory

To my family that have always believed in me.

Acknowledgement

I would like to give my thanks to my professor, Professor Francisco Brójo, for his availability and patience.
Secondly, I would like to thank my parents for the support, emotional, mental and financial, they gave me while I was working and studying for these past six years.
Lastly, I would like to give my thanks to my friends, Rui, José, Beatriz and Nicole for all the help they gave me and all the fun moments that diminish the stress of doing this dissertation.

Resumo

À medida que novos motores são construidos, a necessidade de melhorar os designs aumenta. O projeto preliminar dos bocais é muto importante visto que são um dos componentes que aumenta a velocidade do jato. Existem muitos fatores envolvidos na seleção de bocal propulsivos: a velocidade de cruzeiro pretendida para a aeronave, a altitude de cruzeiro e outros.
Na história da aviação, o projeto preliminar evoluiu desde desenhos em papel para designs digitais, e da mesma maneira, as técnicas utilizadas também mudaram. O método das características foi um dos métodos que ganhou popularidade nos anos oitenta, empregue primeiramente em papel mas depois podendo ser aplicado juntamente com um software de cálculo.
Esta dissertação aplica o Método das Características para fazer o design da parte supersónica do bocal, e descreve como alguns fatores, por exemplo, a altitude, influenciam o contorno do bocal, como objectivo principal.
O Estado da Arte, capítulo 2, introduz uma breve descrição dos tipos de bocais propulsivos que existem e a aplicação de cada um deles.
Os conhecimentos de termodinámica requeridos, desde o básico até ao avançado para conseguir obter os resultados presentes no capítulo 5 são demonstrados no capítulo 3. A fundação teórica explica a relação entre trabalho e calor, a razão de calor específicos, a velocidade do som, o número de Mach, os tipos de fluxo, os choques, a fan de expanção e como as variações de pressão afetam o fluxo de dentro do bocal propulsivo.
O capítulo do método de design demonstra, passo por passo, como se aplica o método das Caracteristrícas, começando por uma introdução do que consiste, de seguida o método linear usado para o design da secção convergente, que é a parte simples, e depois o design da secção divergente, sendo esta a parte complexa. O código, em MATLAB, utilizado para o design, também é explicado passo por passo.
O capítulo dos resultados demostra o que aparece ao utilizador quando inicia o código e os inputs necessários para o código funcionar e fornecer resultados. Três casos são descritos e explicados, para isto algumas variavéis são mudadas para serem observadas as diferenças entre eles.
Os resultados desta dissertação indicam que um bocal propulsivo opera com um fluxo sobre expandido, e que o fluxo na secção convergente nao atinge um estado estrangulado, mas o decrescimento de pressão ao longo do bocal tem um comportamento similar a um fluxo isentrópico, estrangulado e supersónico.

Palavras-Chave

Design, Supersónico, Método das Características, Convergente, Divergente, Bocal.

Abstract

As new engines are built, the necessity of improving the initial design grows. The preliminary design of nozzles is one of the most important parts due to being the component that increases the speed of the flow even more than the rest of the engine. There are a lot of factors involved in the selection of the nozzle: the cruise speed intended for the aircraft, the cruise altitude and others.
As the design methods evolved from paper drafts, in the beginning of the history of aviation, to digital designs, in the present days, the methods employed to do it also changed. The Method of Characteristics was one of the methods that gain some popularity around the 1980's being first used in paper drafts and then with computer software.
This dissertation utilizes the Method of Characteristics to design the supersonic section of the nozzle, and describes how such factors, as the altitude, influence the shape of the contour, as the main goal.
The State of the art, chapter 2, introduces a brief description of the types of nozzles that exist and the application for each one of them.
From the basics of thermodynamics to advanced Aerothermodynamics, it is explained the knowledge required to accomplish the results presented on chapter 5. The theoretical foundation, 3, explains the relationship between work and heat as well as the specific heat ratio, the speed of sound and the Mach number, the types of flow, the shocks, the expansion fans and how the variations of pressure affect the flow inside a nozzle.
The Design method chapter lays out step by step how to apply the Method of Characteristics, starting with an introduction to the method, then a linear method to design the convergent section, requiring only a few step to do it, and the design of the divergent section of the nozzle, which is the hardest part to attain. The code, in MATLAB, behind the design, is also explained step by step.
The Results chapter depicts what appears to the user when initiating the code and what inputs are required for the code to work and give results.There are three cases described and explained, where some variables were changed to observe the difference between those cases.
The results of this dissertation indicated that the nozzle was operating with an overexpanded flow, and the convergent section could not achieve a choked flow at the throat, but the pressure decrease along the nozzle had a similar behavior to a choked isentropic supersonic flow.

Keywords

Design, Supersonic, Method of Characteristics, Convergent, Divergent, Nozzle.

Contents

List of Figures

List of Tables

Nomenclature

A	Area	m^2
a	Speed of Sound	$\frac{m}{s}$
C	Characteristic	
c	Specific Heat Capacity	$\frac{K}{kgK}$
D	Determinant of the Denominator	
E	Energy	J
e	Specific Energy	$\frac{J}{kg}$
F	Thrust	N
H	Enthalpy	J
h	Specific Enthalpy	$\frac{J}{kg}$
K	Riemann Invariant	
L	Length of the Convergent Section	m
M	Mach Number	
$\dot{m}$	Mass Flow	$\frac{kg}{s}$
N	Determinant of the Numerator	
p	Pressure	Pa
Q	Heat	J
q	Specific Heat	$\frac{J}{kg}$
R	Real Gas Constant	$\frac{J}{kgK}$
r	Radius	m
S	Entropy	J
s	Specific Entropy	$\frac{J}{kgK}$
T	Temperature	K
t	Time	s
U	Speed of the Flow	$\frac{m}{s}$
u	Local Speed of the Flow	$\frac{m}{s}$
V	Volume	m^3
v	Specific Volume	$\frac{m^3}{kg}$
x	X axis position	m
W	Work	J
w	Specific Work	$\frac{J}{kg}$
α	Convergent Section Inclination	$^\circ$
β	Inclination Angle	$^\circ$
γ	Specific Heat Ratio	
θ	Expansion Fan Angle	$^\circ$
μ	Mach Angle	$^\circ$
ν	Prandtl-Meyer Angle	$^\circ$
ρ	Density	$\frac{kg}{m^3}$
ϕ	Velocity Potential	

Superscripts

$*$	Critial Value

Subscripts

b	Back/Ambient
e	Outlet/Exit
g	Gross
i	Inlet
max	Total Angle
n	Oblique Shock
p	Constant Pressure Process
s	Shock
t	Throat
v	Constant Volume Process
x	X Axys Position
y	Y Axys Position
0	Stagnation
1	Stage One
2	Stage two
$+$	Left
$-$	Right

Acronyms

PDE	Partial Differential Equation
ODE	Ordinary Differential Equation
MOC	Method of Characteristics
CD	Convergent-Divergent

Chapter 1

Introduction

1.1 Motivation

Since the beginning of the human history, mankind has tried to push itself to higher limits. The need to improve, to be and do better has driven men and women to invent and reinvent themselves in order to achieve some of the great accomplishments, like the Moon landing, technologically speaking.

In 1890, Gustaf de Laval developed the first nozzle that could accomplish supersonic speeds, de Laval nozzle for a steam turbine, that made use of kinetic energy of the steam rather than solely on the pressure, but the machinery of the time could not withstand the temperatures present there. This event carved the path of the modern nozzles in use today in a variety of vehicles, armament and other components that require this sort of technology. The concept of supersonic nozzle has evolved and nowadays there are some derivations that have strong points according to the mission in cause, for example, while subsonic commercial aircraft possesses annular nozzles, the fighter jets possess variable-geometry nozzles.

Since the mission of commercial aircraft requires them to travel long distances at the same altitude, the annular nozzle is the best choice considering that their efficiency is located in a small range of altitudes. This is accompanied by a low complexity, weight and cost comparing with the variable-geometry nozzle of the modern fighter jet which outmatches the flight envelope of the latter.

New technology and the increasing demand for superior performance motivates the purpose of researching new ideas capable of increasing the efficiency and effectiveness of such engines, being the increase in Thrust/Weight ratio and the addition of the lowest weight possible to the engine, the main driving for evolution on this field.

As one of the fields that gives me the most curiosity, it is my belief that there is still room to improve as far as nozzles are concern, such as an alternative to the expensive and complex variable-geometry nozzles retaining the large flight envelope.

1.2 Objectives

The creation of this MATLAB code to compute the design of a supersonic nozzle is a possible step in the improvement of such technology, with the goal of helping future researchers or enthusiasts in their work. The main of goal of this work resides in the design of a axisymmetric, fixed-geometry, convergent-divergent, supersonic nozzle with an optimal expanded flow applying the Method of Characteristics.

Chapter 2

State of the Art

This chapter introduces the nozzles in the context of this work. It is divided into three main sections: the introduction to nozzles, the types of nozzles and the afterburners.
The introduction to nozzles gives a brief explanation of the importance of the referred component, the factors involved in its design and the parts of its structure.
The section of the types of nozzles presents the wide variety of nozzles that exist, how each of them works, respective advantages and disadvantages and examples of aircrafts that use those nozzles.
The afterburner section explains the structure of the afterburner, how it works, when it is activated and examples of aircrafts that use it.

2.1 Introduction to Nozzles

With the advance of technology in all fronts, the exhaust systems suffered a lot of changes throughout the years. Depending on the type of aircraft, the jet of hot gases can play or not a big part on the thrust. For example, on a turbofan engine, the conduct of the flow is rather important while for turbo-propeller engines the exhaust gases are not a significant work force. Having the most important role in the overall thrust of the aircraft, the performance of the nozzle is influenced by a lot of factors that must be optimized, such as, the complexity, reliability, cost, maintainability, length, cooling and the most important one, weight. These factors are conditioned by the type of aircraft and the mission requirement.
The most important features of the exhaust system for non-afterburning engines are the tail cone, the exhaust duct and the exhaust nozzle, and for afterburning engines adds the afterburner pipe.
The objective of the nozzle is to “direct the flow of hot gases rearward to cause a high exit velocity to the gases while preventing turbulence” [11].

2.2 Types of Nozzles

Nozzles may be classified as:

1. Convergent or Convergent-Divergent (C-D) types;
2. Axisymmetric or two-dimensional types;
3. Fixed-geometry or variable-geometry types.

2.2.1 Convergent

Convergent nozzles, Figure 2.1, are some of the most basic nozzles that exist, normally of a fixed-geometry nature, and so, there is no need for control systems and mobile components.

Some designs have variable-geometry as a means to widen the range of performance, instead of restricting it to a single phase of flight, usually the cruise.
In the initial part of the operation, the exit velocity of the gases is subsonic at low-thrust conditions and reaches the speed of sound in most operating conditions [12].
The flow at subsonic speeds is considered incompressible, which leads to an increase in the velocity of the jet. While the area and the static pressure decrease until the throat where it chokes ($\frac{P*}{P_0} = 0.5283$ for $\gamma = 1.4$) and leaves the nozzle at Mach one velocity, the expansion is incomplete, since most of it occurs outside the nozzle, developing a pressure thrust. Even though the expansion is incomplete, in the case of the subsonic aircraft, the use of a convergent$-$divergent nozzle is not worth it since the addition of weight, complexity and increase use of fuel does not justify the change.
Extreme manoeuvring and aircraft speed are not the priorities for subsonic aircraft, so there is no usage of afterburner with convergent nozzles.

Figure 2.1: a319 Convergent nozzle [1].

2.2.2 Convergent-Divergent (CD)

The convergent-divergent nozzle is comprised of a convergent nozzle and the addition of a divergent nozzle, a structure that starts with a small area and grows until a certain bigger area established by the manufacturer. It can have a fixed-geometry or a variable geometry, axisymmetric or non-axisymmetric, depending on the mission that the aircraft is required to do. The type of engine is present on aircraft that need to reach supersonic/hypersonic speed.
The convergent part is where the flow from the engine enters having a certain temperature and pressure.
As explained before, the static pressure and the area decrease while the velocity of the jet increases. When the static pressure reaches a certain critical point where it chokes, $\frac{P*}{P_0} = 0.5283$ for $\gamma = 1.4$, the pressure of the flow exiting the nozzle is greater than the pressure of the surrounding air, which leads to the incomplete expansion of the jet. To solve this problem, the divergent part completes the expansion of the jet. Since for choked flow $Mach > 1$, with an increasing area and compressible flow, the velocity increases, and the remaining pressure drops until it is equal to the ambient pressure. This will lead to an higher momentum thrust instead of a pressure thrust.
Modern engines for supersonic aircrafts are still not capable of developing their own supersonic flow only relying on a convergent-divergent nozzle, so an afterburner is usually introduced with the engine.

2.2.3 Axisymmetric

The axisymmetric nozzles, Figure 2.2, are present in the majority of the engines because they are structurally efficient, less complex and have a longer time of usage, providing an extended technological background in contrast to its counter-part.

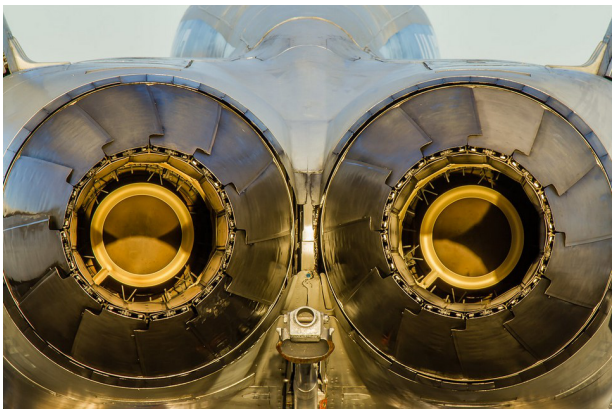

Figure 2.2: F-18 CD nozzle [2].

2.2.4 Non-Axisymmetric

Non-Axisymmetric nozzles are the variety of nozzles that can deflect the flow of hot gases in a different direction than the one before reaching the exhaust.

It is characterized by its heavier and less efficient structure due to the higher complexity, and the lack of technological base, limiting a lot of progress and insight on this area [13].

Typically, the nozzle is round, but recent experiments have led to the development of nozzles with rectangular exits.

The thrust vectoring allows the aircraft to change its course faster than just with conventional control surfaces, such as flaps and ailerons which are unable to contribute as much, particularly at low speeds. Firstly, Non-Axisymmetric nozzles were invented to perform V/STOL (Vertical or Short Take Off and Landing) but their development in the following years led to other variants of the same mechanism, giving modern day aircraft better and faster climb rates.

The thrust vectoring can be divided into two classes, mechanical control and fluidic control. Mechanical control implicates the physical change of the nozzle, for example, the deflection of some plates, which is a heavy and complex system. It is divided in internal thrust that allows pitch control only (Lockheed Martin F-22 Raptor [14], Figure 2.3), and external control that allows pitch and yaw controls (Iris Nozzle Figure 2.6). Fluidic control comprises the infusion or removal of air from the boundary layer of the jet, but has yet to be demonstrated in real life situations.

Figure 2.3: F-22 thrust vectoring nozzle [3].

2.2.5 Fixed-Geometry

The fixed-geometry nozzles require no moving parts or mechanic controls are needed, and by consequence, they are lightweight and less complex.

2.2.6 Variable-Geometry

The variable-geometry nozzles tend to be a lot heavier and complex than the fixed-geometry nozzles. There are three types of nozzles with variable geometry: the Plug nozzles, the Ejectors and the Iris nozzles.

The Plug nozzles are very similar to the inlet spike, they possess a barrel-shaped wall meeting a convergent end inside the plug [15]. The flow starts subsonic ($M < 1$), when the jet meets the plug, the airflow enters the convergent part while contouring the plug and then reaching the throat, where it chokes ($M = 1$). Afterwards, the flow enters the divergent part where it continues to accelerate ($M > 1$).

The plug shape was designed in a way that cancels the expansion waves that can occur, redirecting the flow into the axial direction [14].

One of the advantages of the plug nozzle is its capacity to be truncated, diminishing the length and weight, and maintain a very close performance to the complete plug [15].

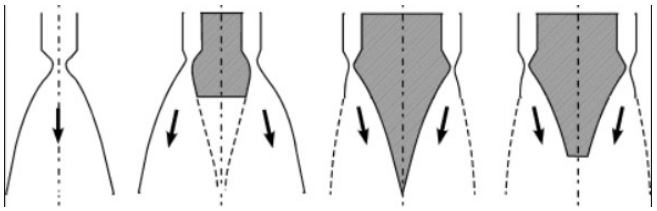

Figure 2.4: Plug nozzle and different truncated plug nozzles [4].

The Ejector type is the simplest of the variable area nozzles. It possesses three different parts: the internal nozzle, the low-pressure chamber and the diffuser, which is the component where the area changes.

Observing figure 2.5, at subsonic speeds, the low-pressure bypass air (secondary airflow) is inserted back into the nozzle constricting the exhaust to a convergent shape, as the jet builds up speed, the two nozzles form a convergent-divergent shape, which augments the velocity of the jet even more.

Although, it is more reliable than the others, it also produces more secondary airflow drag and is considerably more inefficient than advanced designs. Some of the most known aircraft used this

type, for example, the Lockheed SR-71 Blackbird, BAC/Aerospatiale Concorde and the General Dynamics F-111 [14].

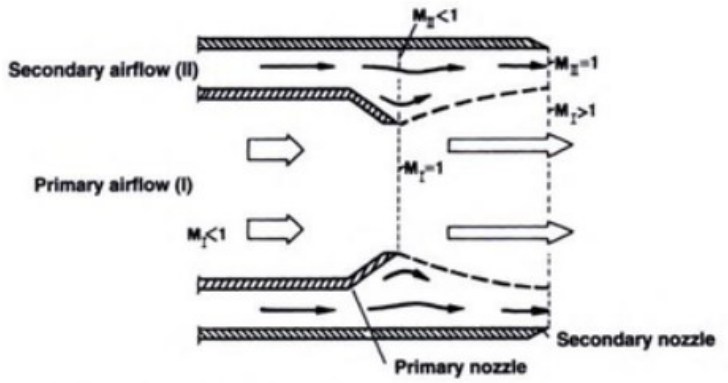

Figure 2.5: Ejector nozzle[5].

The Iris nozzle is commonly used in modern fighter jets and bombers since its mechanics are more qualified for extreme manoeuvring and it is capable of enhancing the altitude range in order to maximize the performance, as well as, the possibility of being combined with thrust-vectoring, if desired.
It is comprised of several overlapping “petal” like structures that adjust the area of the exhaust shown in figure 2.6, extending or retracting to the desired area, a system that is far more complicated than the two previous ones.
The pioneer use of the Iris nozzle was in the Grumman F-14 variant B and later to the McDonnell Douglas F-15 Eagle and the General Dynamics F-16 [14].

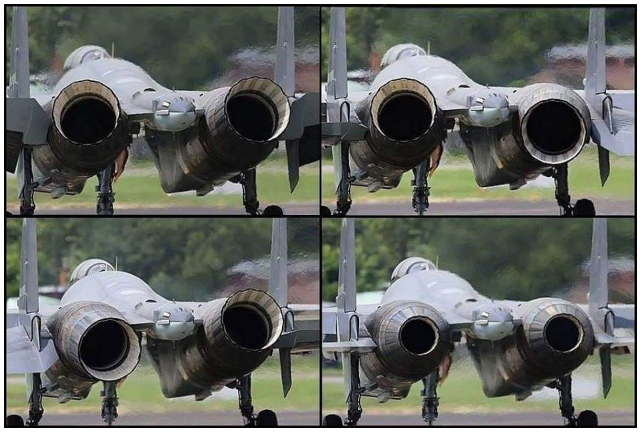

Figure 2.6: Iris nozzle of a Su-35 [6].

2.3 Afterburner

The Afterburners are mostly used in military aircraft with turbofan and turbojet engines, some exceptions are the BAC/Aerospatiale Concorde and the Tupolev Tu144 [12].
The afterburner adds weight and stagnation pressure losses, however it remains as a better solution than the increase in the dry thrust of the engine itself, which would lead to a substantial weight and complexity increment to the engine.

Due to temperature limitations in the combustion chamber, a portion of the oxygen in the air is not used in the combustion in the combustion chamber and can be used later on the afterburner, adding more fuel, igniting it and extracting more energy to increase the velocity of the exhaust gases, thus increasing the thrust [12].
The Afterburner is comprised of a diffuser, the spray bars, a flame holder and the afterburner pipe, the last two components can be seen in Figure 2.7.
The diffuser is the component that connects the low-pressure turbine and the afterburner pipe and has the main goal of slowing down the flow. This is required because the flame stabilization is a complicated aspect to control with higher flow velocities.
The spray bars are located inside the afterburner pipe. Their main goal is to spray the fuel transversely to the flow, which needs to be evaporated so the hot gases coming from the turbine may reduce it into smaller droplets, leaving the flame holder to ignite the mixture. The flame holder is located in front of the spray bar. To avoid the blow out of the engine, where the flame propagates slower than the flow that comes from upstream, the flame holder sets up a recirculation zone that keeps the mixture ignited, this process just needs a small amount of time to stabilize the flame so it can be switched off afterwards [12].
The afterburner pipe is the main feature of the afterburner as a whole, it is placed between the diffuser and the nozzle. The length of the pipe is determined by the time of the combustion of the mixture to release the desired amount of energy that can be extracted. This needs to be balanced with weight increase and friction losses. The afterburner is comprised of the inner and outer cases. Between them a secondary flow passes through and exits through small holes along the inner case providing a cooling boundary, so the metal doesn't melt.
During the time that the afterburner is on, the consumption rate of fuel dramatically increases, as a means to use the remaining oxygen in the area. Meanwhile the nozzle area has a variation of 50 percent to 150 percent from non-afterburning to full afterburning operation [12].
When an engine is equipped with an afterburner, the nozzle is, in most cases, a convergent-divergent with variable geometry, combining the increase in thrust with nozzle throat/exit area control in order to perform supersonic flight or high speed manoeuvring.

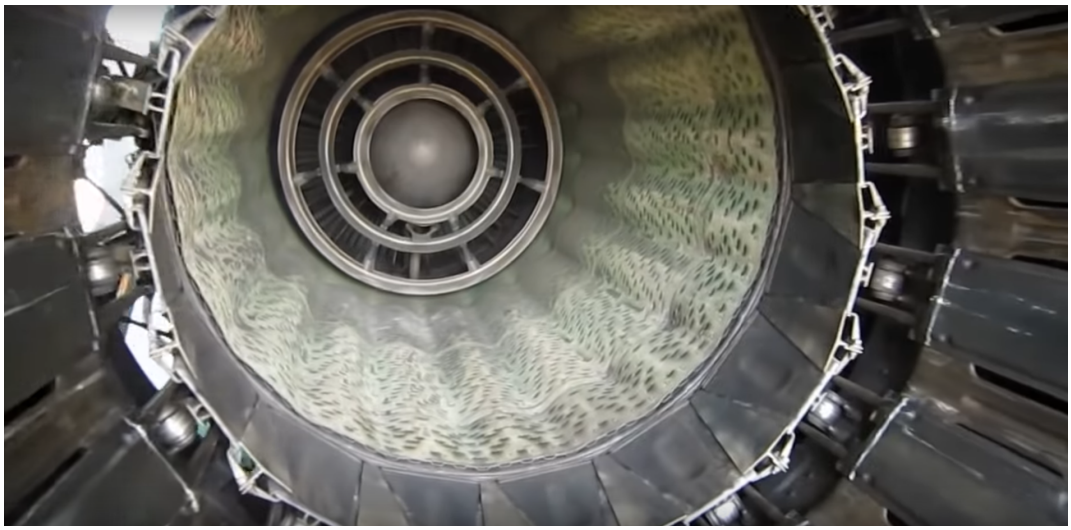

Figure 2.7: Afterburner of a J79 Turbojet [7].

Chapter 3

Theoretical Foundation

3.1 Introduction

In order to accomplish this dissertation, the theoretical foundation behind all the work is demonstrated in this chapter through existing mathematical concepts.
This chapter is composed of seven sections: Thermodynamics and Applications, Types of flow, Flow inside a Convergent-Divergent Nozzle, Normal Shock, Oblique Shock, Prandtl-Meyer Expansion Fan and Cases of Gas Regimes and occurring phenomena.
The Thermodynamics and Applications section presents the basis that sustains this dissertation, the basic concepts of the equations of energy, work, heat and their connection. Besides these, there is reference to the specific heat constant, the speed of sound, Mach number and their importance as main concepts of the functions that are used in the code.
The types of Flow present the behaviour and characteristics of each flow and the relation with the following sections.
The Flow inside a Convergent-Divergent Nozzle sections introduces the assumptions made in order to ease the calculations, the laws behind the flow, and how the area change affects the speed of the stream.
The Normal Shock section depicts the characteristic of a normal shock, the conditions needed to happen and the consequences, on various locations inside the nozzle.
The Oblique shock sections has the same structure of the Normal Shock section.
The Prandtl-Meyer expansion fan section presents the principles of an expansion fan, how it is composed, its characteristics and how to compute the various angles using the functions presented.
The Cases of gas regimes and occurring phenomena shows how the pressure inside a nozzle affects the flow. This section explains the flows that can occur inside a nozzle with a variation of the ambient pressure and how it affects the performance of the nozzle.
The Theoretical chapter is the ground foundations for the Design chapter.

3.2 Thermodynamics and Applications

The term energy is present in the everyday life of every person; however, its definition is still being discussed nowadays. The closest to a definition that currently exists is: “Energy is usually defined as the ability to do mechanical work”. Energy can be subdivided into two types of energy: energy in transition and energy reserved inside a mass. Heat and work are part of the first type, they can shift between substances due to a driving potential. The kinetic and potential energy belong to the second type.
In thermodynamics, the main concern is the change in internal energy rather than its absolute value. According to the first law of thermodynamics, the energy within an isolated system (our universe) cannot be destroyed, only transformed.

The International unit (SI) for the different types of energy is the Joule (J), which is equal to the work done by a one-newton force acting over a one-meter distance.

$$de = \partial q + \partial w \quad (3.1)$$

The energy within a system can only be increased or decreased by heat or work [8]. If heat is added to or work is done on the system, the energy increases. If heat is removed from the system or work is done by it, the energy decreases.

3.2.1 Work

The work can be described, as seen in the equation (3.2), as the variation of volume with constant pressure. When the system does work on the outside the volume diminishes, inversely, when the system is worked by the outside the volume increases [12].

$$\partial w = -pdv \quad (3.2)$$

Introducing the work equation (3.2) on the energy equation (3.1), one can get:

$$de = \partial q - pdv \quad (3.3)$$

This equation relates the energy of a system with the work.

3.2.2 Heat

Heat is a spontaneous flow of thermal energy between a body with a higher temperature to another one with a lower temperature.
The enthalpy plays a huge part on the description of heat [12].
Enthalpy is a thermodynamic property, defined by the sum of internal energy and the product of pressure and volume of system [16]; this expresses the capability to do non-mechanical work and the capability to release heat:

$$H = E + pV = E + nRT \quad (3.4)$$

Being the specific enthalpy [8]:

$$h = e + pv = e + RT \quad (3.5)$$

Using the perfect gas law, the equation changes depending on the objective on hand. Deriving the first part of (3.5), the following equation is obtained:

$$dh = de + pdv + vdp \quad (3.6)$$

And introducing the energy equation attained from the work section (3.3):

$$de = \partial q - pdv \quad (3.7)$$

The heat equation is obtained in terms of enthalpy:

$$\partial q = dh - vdp \quad (3.8)$$

3.2.3 Specific Heat Capacity

The specific heat constant is the amount of energy, for each substance, that needs to be provided to raise one kilogram of that substance, one degree Kelvin.

$$c = \frac{\partial q}{dT} \quad (3.9)$$

For a fixed ∂q, the resulting dT depends on the process.

3.2.3.1 Constant Pressure and Constant Volume

There are two processes in which we can identify the conditions in cause, in the subject of energy transfer: the constant pressure process and the constant volume process [8].
The constant pressure process is given by:

$$c_p = \left(\frac{\partial q}{dT}\right)_p \iff \quad (3.10)$$

$$\iff \partial q = c_p dT$$

$$\iff dh = c_p dT$$

$$\iff h = c_p T \quad (3.11)$$

The constant volume process is given by:

$$c_v = \left(\frac{\partial q}{dT}\right)_v \iff \quad (3.12)$$

$$\iff \partial q = c_v dT$$

$$\iff de = c_v dT$$

$$\iff e = c_v T \quad (3.13)$$

3.2.3.2 Specific Heat Ratio

The specific heat ratio is the ratio between the heat capacity at constant pressure and heat capacity at constant volume [8].

$$\gamma = \frac{c_p}{c_v} \quad (3.14)$$

For an ideal gas, the heat capacity is constant with variations of temperature.

3.2.4 Speed of Sound

The speed of sound is a measurement of a disturbance (wave) travelling a certain distance per time unit through a medium (solid, liquid or gaseous), it is an isentropic process. Since the speed of sound depends on the collision of molecules, it will be subject to the state of the medium and, considering an ideal gas it will only depend on the temperature. The speed of sound is given by:

$$a = \sqrt{\gamma RT} \quad (3.15)$$

In the SI unit system, it is measured as m/s.

3.2.5 Mach Number

The Mach number represents the ratio between the local speed of the flow and the local speed of sound, as seen in equation (3.16). The Mach number can also be used to determine if a flow is compressible or incompressible.

$$M = \frac{u}{a} \quad (3.16)$$

There are four distinct types of characterization regarding the Mach number:

1. $M < 1$, Subsonic flow, the compressibility effects can be neglected at lower subsonic speeds, around Mach 0.3, mostly found in Convergent nozzles;
2. $M = 1$, Sonic flow, mostly found in the throat region, that becomes a critical area [14];
3. $M > 1$, Supersonic flow, mostly present in the Divergent section of the nozzle;
4. $M > 5$, Hypersonic flow.

3.3 Types of Flow

3.3.1 Quasi One-Dimensional Flow

Quasi One-Dimensional flow happens when the properties of the stream only change in one direction. If such variation is gradual, then the changes taking place in cross stream directions can be neglected [16].

3.3.2 Incompressible Flow

Incompressible flow is a type of flow which the pressure variations do not affect the density, thus the density is constant throughout the stream. It can also be said that in an incompressible flow the jet speed is low enough to be called negligible compared to the speed of sound [9]. Normally, in terms of Mach number, incompressible flow goes from Mach 0 to Mach 0.3 [8],

where the variations of density are no longer insignificant to an analysis of the flow. The two properties that are mainly involved in the study of incompressible flow are the velocity and the pressure, hence the equations of momentum and conservation of mass are used in problems of this kind.

3.3.3 Compressible Flow

Inversely to the incompressible flow, in the compressible flow the pressure variations affect the density of the flow. The density becomes part of the unknown properties of the flow along with the temperature, being necessary the use of the equation of the perfect gases and the conservation of energy. In terms of Mach number, compressible flow starts around Mach 0.3 and occurs between the two extremes of isothermal and adiabatic conditions.

3.3.4 Isentropic Flow

The isentropic flow is an idealized flow used to compare with real flows as a means to simplify calculations, it is composed of both adiabatic and reversible processes.

3.3.4.1 Adiabatic Process

An adiabatic process occurs when there are no transfers of energy in the form of heat or transfers of matter between the flow and the surroundings, which in this case, is the nozzle wall. This process is considered since after the heating of the wall to match the flow temperature, the overall temperature remains roughly the same [9]. The change in internal energy can only be due to the work done on or by the system, thus (3.17). The temperature can only change due to the changes of density.

$$\partial q = dh - vdp = 0 \quad (3.17)$$

$$h_1 + \frac{V_1^2}{2} = h_2 + \frac{V_2^2}{2} \iff \quad (3.18)$$
$$\iff h + \frac{V^2}{2} = constant$$

$$PV^\gamma = constant \quad (3.19)$$

Since the entropy of the system is constant, the flow becomes frictionless and the work is simply a consequence of pressure and volume, as observed in equation (3.19).

3.3.4.2 Reversible Process

A reversible process is an idealized process that occurs when the properties of the flow can be brought back to their original state. Throughout this, the flow is in thermodynamic equilibrium with its wall.

3.3.4.3 Isentropic Process

Isentropic means that the system has constant entropy, so, the variations of entropy are neglected, which is a direct consequence of the flow being both adiabatic and reversible, by the second law of thermodynamics, due to a small and gradual change in the flow. This type of flow provides important relations of thermodynamics variables along the entire nozzle. Here, the total pressure and temperature are constant through the nozzle.
Some of those relations are presented below:

$$\frac{P_2}{P_1} = \left(\frac{\rho_2}{\rho_1}\right)^{\gamma} = \left(\frac{T_2}{T_1}\right)^{\frac{\gamma}{\gamma-1}} \quad (3.20)$$

$$p_1 + \frac{1}{2}\rho V_1^2 = p_2 + \frac{1}{2}\rho V_2^2 \quad (3.21)$$

Isentropic processes can be considered for both incompressible and compressible flows. Even though the specific heat ratio is a function of the temperature in an isentropic flow, it remains constant since it still gives a good approximation to real cases in initial assessments.

3.4 Flow inside a Convergent-Divergent Nozzle

3.4.1 Equations of State

Some assumption must be made in order to simplify the flow throughout the nozzle, idealized flow, this will give a good first approximation to the real cases [14].

1. The flow entering and leaving through a nozzle is steady and quasi-one-dimensional [14];
2. The entrance and exit stations are in pressure equilibrium with the surroundings, $p_0 = p_e$ [14];
3. There is no heat transfer across the boundaries of the nozzle (wall) and the surroundings [14];
4. The frictional forces are negligible throughout the nozzle [14];
5. The mass flow is constant through the nozzle [14].

3.4.1.1 Perfect Gas Law

The idealized flow behaves under the perfect gas law [8]:

$$pV = nRT \quad (3.22)$$

And in its differential form:

$$\frac{dp}{p} = \frac{dT}{T} - \frac{dV}{V} \quad (3.23)$$

3.4.1.2 Momentum Conservation Equation

Introducing the momentum conservation equation, by Newton's second law, the variation in momentum of the fluid inside the nozzle is equal to the force acting on the fluid.

$$dp = -\rho u du \quad (3.24)$$

3.4.1.3 Mass Conservation Equation

Introducing the mass conservation equation, the mass addition or subtraction is negligible, the variation of mass flow is zero, this meaning that the mass flow that enters the nozzle is the same that leaves the nozzle.

$$\frac{d\rho}{\rho} + \frac{du}{u} + \frac{dA}{A} = 0 \quad (3.25)$$

Combining the perfect gas law with the mass conservation equation with Mach number:

$$\dot{m} = pAM\sqrt{\frac{\gamma}{RT}} \quad (3.26)$$

3.4.2 Flow through the nozzle

Starting with the divergent section of the nozzle, and assuming that for Mach numbers lower than one all flow is incompressible, with the mass conservation equation, and knowing that the flow is incompressible flow, $d\rho = 0$:

$$\frac{du}{u} = -\frac{dA}{A} \quad (3.27)$$

Taking from this equation two different cases can be analysed:

1. For a decrease in area we have an increase in velocity;

$$dA < 0 \qquad du > 0$$

2. For an increase in area we have a decrease in velocity.

$$dA > 0 \qquad du < 0$$

Making use of both the momentum conservation and the mass conservation the changes in a divergent-convergent nozzle can be analysed, taking into account the previous examinations of compressible flow for the convergent section and making a connection with the divergent section of the nozzle, which is going to be explained in the forthcoming equations. To accomplish this, the pressure needs to be a function of density and entropy:

$$p = f(\rho, s) \quad (3.28)$$

$$dp = \left(\frac{\partial p}{\partial \rho}\right)_s \partial\rho + \left(\frac{\partial p}{\partial s}\right)_\rho \partial s \quad (3.29)$$

Assuming the flow is isentropic, the changes in entropy are null, $ds = 0$, and results in:

$$\frac{dp}{\partial \rho} = \left(\frac{\partial P}{\partial \rho}\right)_s = a^2 \quad (3.30)$$

With the relation between the pressure and the speed of sound, one can reach an equation to correlate density and local Mach number:

$$\begin{aligned} &\frac{dp}{\rho} = a^2 \frac{d\rho}{\rho} \iff \\ &\iff -udu = a^2 \frac{d\rho}{\rho} \\ &\iff \frac{d\rho}{\rho} = \frac{-u^2}{a^2}\frac{du}{u} \\ &\iff \frac{d\rho}{\rho} = -M^2 \frac{du}{u} \end{aligned} \quad (3.31)$$

Combining the mass conservation equation with equation (3.31), it results in a relation between area and Mach number:

$$\begin{aligned} &-\frac{du}{u} - \frac{dA}{A} = -M^2 \frac{du}{u} \iff \\ &\iff \frac{dA}{A} = [M^2 - 1]\frac{du}{u} \end{aligned} \quad (3.32)$$

From equation (3.32) the following can be established:

1. An increase in area is proportional to an increase in velocity.

$$dA > 0 \qquad du > 0$$

2. For a decrease in area, there is a decreasing velocity.

$$dA < 0 \qquad du < 0$$

3.4.3 Gross Thrust

The gross thrust of the nozzle can be computed using equation 3.33 [9].

$$Fg = A_e[p_e(1 + \gamma M_e^2) - p_b] \quad (3.33)$$

3.5 Normal shock

In the matter of explaining normal shocks there is a need to assume certain aspects about the flow. The flow must be steady, adiabatic, inviscid and no external forces must be exerted in the

control body [8].
In a steady flow the fluid properties do not change over time, they remain constant throughout.

$$\frac{\partial}{\partial t} = 0 \quad (3.34)$$

As explained in subchapter 3.3.4.1, the flow is adiabatic when there is no transfers of heat. The increase in temperature across a normal shockwave is a result of the transfer of kinetic energy into internal energy.
The viscous forces are neglected since the wave is considered to be inside the control body.
Normal shocks are phenomena where the entropy changes across the wave so, they are particularly different from isentropic phenomena. A normal shock can only occur in a supersonic flow [8].
The equations below are the governing equation for one dimensional, steady, adiabatic and inviscid flow [8]:

$$M_2^2 = \frac{(\gamma-1)M_1^2 + 2}{2\gamma M_1^2 - (\gamma-1)} \quad (3.35)$$

$$\frac{T_2}{T_1} = \left[\frac{2}{(\gamma+1)M_1^2} + \left(\frac{\gamma-1}{\gamma+1}\right)\right]\left[\left(\frac{2\gamma}{\gamma+1}\right)M_1^2 - \left(\frac{\gamma-1}{\gamma+1}\right)\right] \quad (3.36)$$

$$\frac{p_2}{p_1} = \left[1 + \left(\frac{2\gamma}{\gamma+1}\right)(M_1^2 - 1)\right] \quad (3.37)$$

The pressure ratio (3.37) can be used as a tool to analyse the shock strength.

$$\frac{\rho_2}{\rho_1} = \left[\frac{(\gamma+1)M_1^2}{2 + (\gamma-1)M_1^2}\right] \quad (3.38)$$

$$\frac{p_{0,2}}{p_{0,1}} = \left[\frac{(\gamma+1)M_1^2}{2 + (\gamma-1)M_1^2}\right]^{\frac{\gamma}{\gamma-1}}\left[\left(\frac{2\gamma}{\gamma+1}\right)M_1^2 - \left(\frac{\gamma-1}{\gamma+1}\right)\right]^{-\frac{1}{\gamma-1}} \quad (3.39)$$

From the stagnation pressure ratio, one can observe that the lower the upstream Mach number, the lower the change in stagnation pressure, and the bigger the upstream Mach number, the bigger the loss of pressure.
The stagnation temperature is constant across a normal shock.

$$T_{0,1} = T_{0,2}$$

$$\frac{p_{0,2}}{p_{0,1}} = e^{-\frac{(s_2 - s_1)}{R}} \quad (3.40)$$

From equation (3.40), one can observe that the stagnation pressure decreases across a normal shock.

Even though in the equations above only the supersonic path is being considered, mathematically a subsonic solution could be found too, but resorting to the second law of thermodynamics, it can be seen that the subsonic solution is not viable, this is demonstrated with the following equations:

$$s_2 - s_1 = c_p \ln \frac{T_2}{T_1} - R \ln \frac{p_2}{p_1} \quad (3.41)$$

$$s_2 - s_1 = c_p \ln \left(\left[1 + \frac{2\gamma}{\gamma+1}(M_1^2 - 1) \right] \frac{2 + (\gamma-1)M_1^2}{(\gamma+1)M_1^2} \right) - R \ln \left[1 + \frac{2\gamma}{\gamma+1}(M_1^2 - 1) \right] \quad (3.42)$$

$$s_2 - s_1 \geq 0 \quad (3.43)$$

Equation (3.43) impels that the entropy increases across a normal shock if the Mach number is bigger than 1 and if the Mach number is equal to 1 the entropy remains constant, being those the two solutions allowed by the second law of thermodynamics.

$$\frac{p_{0,2}}{p_{0,1}} = e^{-\frac{(s_2 - s_1)}{R}} \quad (3.44)$$

From equation (3.44), one can notice that the stagnation pressure decreases across a normal shock.
In conclusion, across a normal shock wave, the pressure, density and temperature increase, and, on the contrary, the velocity decreases and the Mach number decreases to a subsonic value.

3.6 Oblique shock

In nature, the most common form of shockwaves comes in the form of oblique shocks [8]. For example, when an airplane is flying at supersonic speeds, using special image capture we can see the oblique shocks coming from the tip of the nose, Figure 3.1 represents an oblique shock over a corner, on the left side. The oblique shocks, as the name states, are shocks with an inclination in respect to the upstream flow direction [12], being this angle β_s, deflecting the course of the flow with an angle θ_s. The angle θ_s in nozzles is usually given by the geometry of the boundary, since the flow next to the boundary needs to be tangent to it. Normal shocks are a special case of the oblique shocks, considering that an oblique shock has an inclination angle of 90^o . The flow prior to the shock is always supersonic and the shock itself has two possible paths, it can be a strong oblique shock (β_s has higher values) , where the flow downstream of the shock is subsonic, or it can be a weak oblique shock (β_s has lower values), where the Mach number still decreases but the flow remains supersonic. Every upstream Mach number is associated with a maximum deflection angle. If the deflection angle is bigger than maximum deflection angle, the shock detaches itself from the wall and a detached bow shock is formed. Oblique shocks occur when the nozzle is overexpanded, this will be explained further below in the subsequent chapters. The calculations of the ratios in oblique shocks are very similar to normal shocks, the tangential components of the velocity are equal, and only the normal

components are calculated using the equations:

$$M_{n,1} = M_1 \sin \beta_s \quad (3.45)$$

Here $M_{n,1}$ replaces M_1 in the equations for normal shock.

$$M_{n,2} = M_2 \sin \beta_s - \theta_s \quad (3.46)$$

Here $M_{n,2}$ replaces M_2 in the equations for normal shock.
The oblique shock relations are the following [8]:

$$M_{n,2}^2 = \frac{1 + \frac{\gamma-1}{2} M_{n,1}^2}{\gamma M_{n,1}^2 - \frac{\gamma-1}{2}} \quad (3.47)$$

$$\frac{\rho_2}{\rho_1} = \frac{(\gamma+1) M_{n,1}^2}{2 + (\gamma-1) M_{n,1}^2} \quad (3.48)$$

$$\frac{p_2}{p_1} = 1 + \frac{2\gamma}{\gamma+1}(M_{n,1}^2 - 1) \quad (3.49)$$

$$\frac{T_2}{T_1} = \frac{p_2}{p_1}\frac{\rho_2}{\rho_1} \quad (3.50)$$

$$T_{0,1} = T_{0,2}$$

$$\frac{P_{0,2}}{P_{0,1}} = \left[\frac{(\gamma+1) M_{n,1}^2}{(\gamma-1) M_{n,1}^2 + 2}\right]^{\frac{\gamma}{\gamma-1}} \left[\frac{\gamma+1}{2\gamma M_{n,1}^2 - (\gamma-1)}\right]^{\frac{1}{\gamma-1}} \quad (3.51)$$

$$M_2 = \frac{M_{n,2}}{\sin \beta_s - \theta_s} \quad (3.52)$$

$$\tan \theta_s = 2 \tan^{-1} \beta_s \frac{M_1^2 \sin^2 \beta_s - 1}{M_1^2(\gamma + \cos 2\beta_s) + 2} \quad (3.53)$$

The equation (3.53) is named the $\theta\beta M$ relation [8] and is the main tool of analysis of oblique waves, the connotations of weak and strong shock come from this equation. A very important factor of oblique shocks is the Mach angle:

$$\mu = \sin^{-1} \frac{1}{M} \quad (3.54)$$

A Mach wave is another part of the oblique shocks and can be defined as an infinitely weak shock.

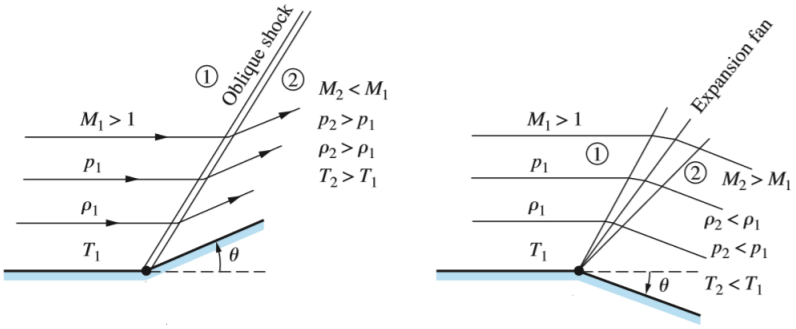

Figure 3.1: Supersonic flow over a corner. [8]

3.7 Prandtl-Meyer expansion fan

Expansion waves are the counterpart of oblique shocks. Instead of reducing the velocity of the stream, they increase the velocity of the stream and respective Mach number while decreasing the static temperature, pressure and density as seen in Figure 3.1 on the right side. In the case of expansion waves the flow is "turned away from itself" [8]. An expansion wave, also called expansion fan, is comprised of an infinite number of weak Mach waves, since each of these Mach waves are isentropic, the whole phenomenon is isentropic, so the isentropic relations can be used to solve problems involving expansion fans, and the stagnation properties are constant. In each of these weak Mach waves, the flow angle changes slightly, assuming a calorically perfect gas, the Prandtl-Meyer function is derived with which the Prandtl-Meyer angle is acquired. The Prandtl-Meyer function is used to calculate the Mach number downstream of the flow.

$$d\theta = \sqrt{M^2 - 1}\frac{dV}{V} \quad (3.55)$$

Equation (3.55) relates the infinitesimal change in velocity dV to the infinitesimal deflection d across a wave of vanishing strength [8]. Deriving the equation above, the Prandtl-Meyer function is obtained [8]:

$$\nu(M) = \sqrt{\frac{\gamma+1}{\gamma-1}}arctan\left(\sqrt{\frac{\gamma-1}{\gamma+1}(M^2-1}\right) - arctan\left(\sqrt{M^2-1}\right) \quad (3.56)$$

Equation (3.57) determines the angle of the expansion fan, it is the angle from the first Mach wave, where Mach is M_1, up until the last Mach wave, where Mach is M_2.

$$\theta = \nu(M_2) - \nu(M_1) \quad (3.57)$$

Each of the weak Mach waves that composed the expansion fan possesses an angle with the direction of flow called Mach angle [14]. This angle is obtained with the equations (3.58) and (3.59), being μ_1 the angle of the first wave and μ_2 the angle of the last wave:

$$\mu_1 = \sin^- 1 \frac{1}{M_1} \quad (3.58)$$

$$\mu_2 = \sin^- 1 \frac{1}{M_2} \quad (3.59)$$

Expansion waves occur when the nozzle is underexpanded, which is explained in the next chapters.

3.8 Cases of gas regimes and occurring phenomena

The flow that passes through a nozzle can be divided in some cases depending on the velocity of the jet [9]. These examples have been made considering a regular de Laval nozzle, but all of them apply to the other varieties of convergent-divergent nozzles that exist, since all of them possess a convergent part, a throat and a divergent part.

There are several different types of flow that can be present inside a convergent-divergent nozzle. To explain what happen inside the nozzle, a figure of the nozzle and a graphic have been made for each type of flow. The plot correlates a pressure ratio between the static pressure along the nozzle, p, and the stagnation pressure, p_0, in the entrance of the nozzle (y axis) and the distance along the nozzle (x axis).

It should be noted that p_0 is going to be considered a fixed value and the value of p_b is the one that changes, in order to simplify the interpretation. The regimes below follow an increase in altitude being the reason that p_b decreases but can also be established for levelled flight where p_0 increase and the p_b is fixed. The throat area A_t is only considered $A*$ when the flow is choked, the star means that it is a critical value only achievable at choked conditions, the same happens with the temperature and the pressure at the throat. It can be observed other values in the following figures and graphics, p_e the pressure at the exit plane, A_e the area of the exit plane and p_b the ambient pressure outside the nozzle. The specific heat ratio is considered as 1.4 [14].

3.8.1 Non-existent Flow

In this case, observing Figure 3.2, the ambient pressure P_b and the pressure entering the nozzle P_0 have the same value, since there is no variation in pressure, the thrust that was supposed to be produced does not exist [14]. The following can be observed:

$$p_0 = p_e = p_b$$

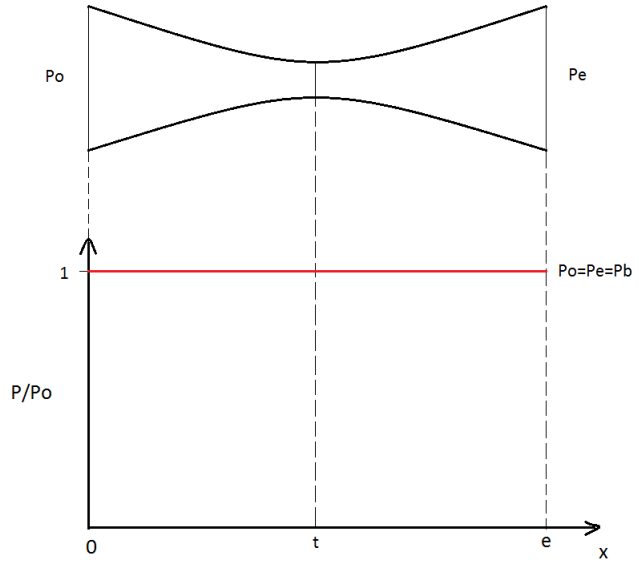

Figure 3.2: Pressure ratios along a CD nozzle considering a situation of no flow.

3.8.2 Isentropic Subsonic Flow

The Isentropic Subsonic flow happens when p_b drops lower than p_0, as seen in Figure 3.3. A jet starts to flow throughout the nozzle and a pressure differential is established producing thrust. In the convergent section, considering subsonic flow, the area of the nozzle is decreasing thereby resulting in an increase of the velocity of the flow and a decrease of pressure until the flow reaches the throat, where it attains the lowest pressure and highest velocity [14].
When the jet enters the divergent section, the area increases, the pressure increases and the velocity decreases. Upon the flow arriving at the exit, the pressure p_e is equal to p_b, but still lower than p_0.

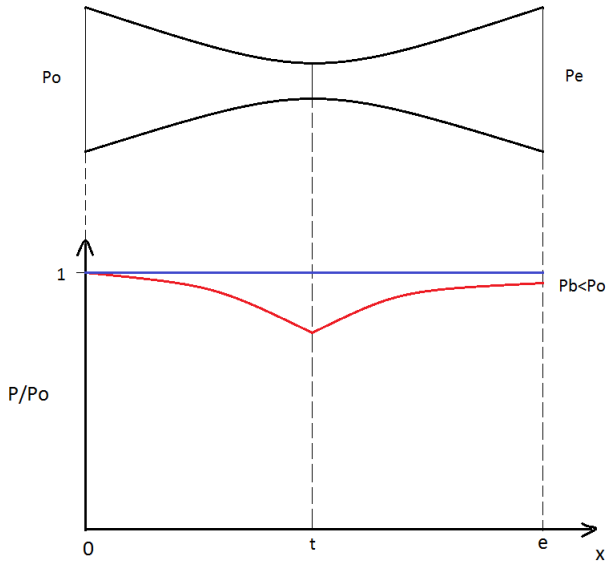

Figure 3.3: Pressure ratios along a CD nozzle considering a situation of Isentropic Subsonic flow.

It should be added that there is more than one solution for p_e. If the velocity of the jet at the throat remains below Mach 1, the subsonic flow throughout the nozzle will keep on happening.

3.8.3 Choked Isentropic Subsonic Flow

Decreasing even more the p_b, the flow is going to increase in velocity, meaning that the ratio of pressures between the entrance of the nozzle and the throat will peak at approximately 0.53, represented in Figure 3.4 by $p*/p_o$, and the speed to Mach one and the flow will be choked. The path of pressures ratio will not change throughout the next regimes on the convergent part of the nozzle.
In this case the back pressure is not low enough for the flow to acquire supersonic speed in the divergent section [14].
After the throat, as stated before, using the relation of area in the divergent section and the throat area and subsequently discovering the Mach in the that area, two different solutions, a subsonic one and a supersonic one, are found. The subsonic path will be further explained below.

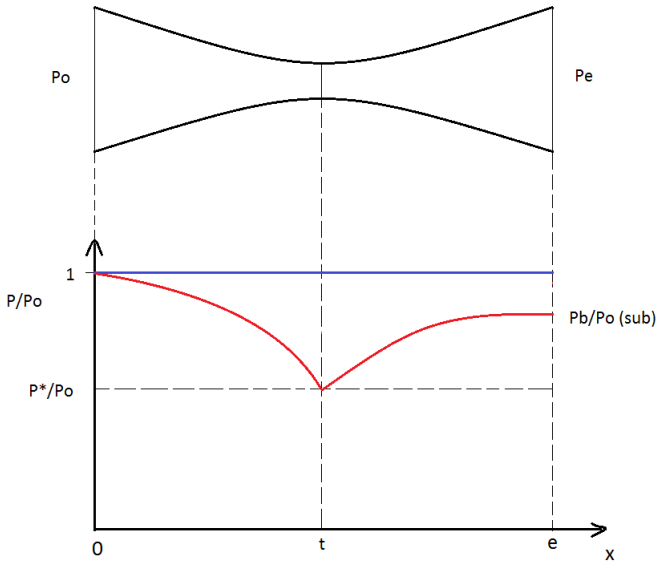

Figure 3.4: Pressure ratios along a CD nozzle considering a situation of Choked Isentropic Subsonic flow.

3.8.4 Choked Isentropic Supersonic Flow

Taking the supersonic path solution after the throat, the flow of the jet will be subsonic in the convergent section, sonic at the throat and supersonic in the divergent section. The back pressure is pulled further down than in the previous case, and the supersonic flow in the divergent part of the nozzle is achieved [14], as seen in Figure 3.5.

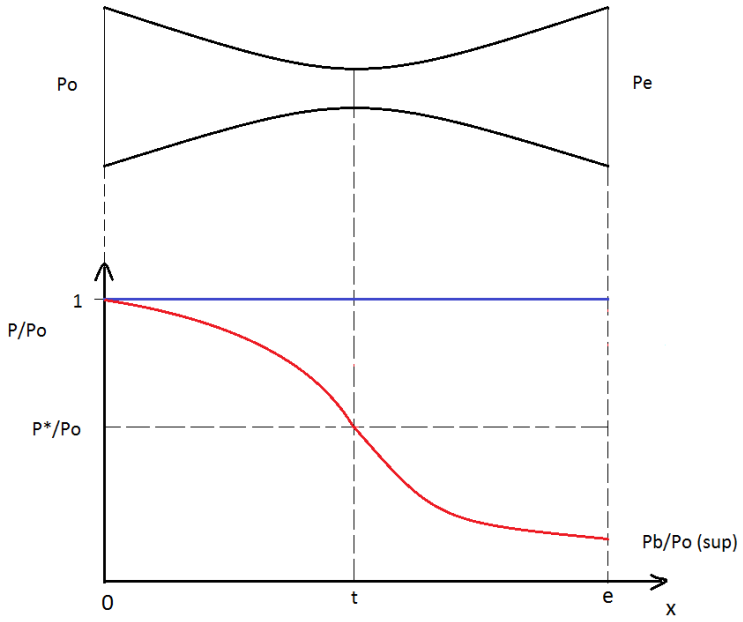

Figure 3.5: Pressure ratios along a CD nozzle considering a situation of Choked Isentropic Supersonic flow.

The next sub-chapters are all derived from this regime. They represent phenomena that might happen during choked isentropic supersonic flow.

3.8.5 Normal Shock inside the Nozzle

The normal shock in a nozzle occurs, normally, in the divergent part and it is a non-isentropic phenomenon. While the flow is supersonic in the divergent part, p_b is too high. To equalize the pressure still inside the nozzle a shock takes place, Figure 3.6, increasing the static pressure p inside the nozzle and decreasing its velocity, the flow after a shock is always subsonic and with the extending area the flow keeps slowing down [14]. The location of a normal shock depends on p_b, the lower the pressure, further downstream is the shock.

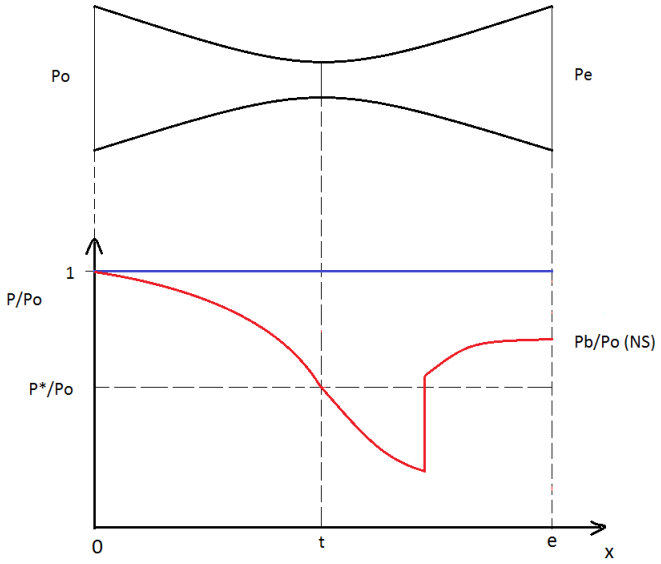

Figure 3.6: Pressure ratios along a CD nozzle considering a situation of Normal shock inside the nozzle.

3.8.6 Normal shock at the exit plane

Pushing the shock further downstream, decreasing p_b, it will result in a normal shock in the exit plane of the nozzle. Until the exit plane, the flow is going to be subsonic, sonic and then supersonic, respectively, without suffering pressure oscillations.

The normal shock occurs in the exit plane as a means to match p_b with p_e, seen in Figure 3.7.

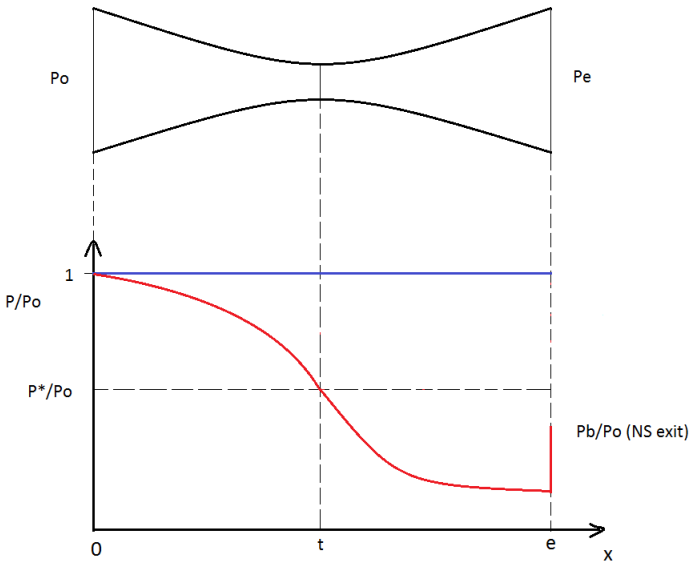

Figure 3.7: Pressure ratios along a CD nozzle considering a situation of Normal shock in the nozzle exit plane.

3.8.7 Overexpanded Flow

Overexpanded flow takes place when the ambient pressure is lower than what it was for a normal shock at the exit, but higher than the ambient pressure for a choked isentropic supersonic flow. In simple terms, the nozzle expanded the jet too much in an effort to match the pressure inside the nozzle and the ambient pressure [14]. Since p_e is lower than p_b, but not sufficiently high for a normal shock to occur inside the nozzle, the pressure exiting the nozzle is going to increase due to weak oblique shock outside the nozzle [10], Figure 3.8.

To straighten out the flow outside the nozzle and match pressures, the flow goes through a sequence of oblique shocks and expansion fans generating what is called shock diamonds.

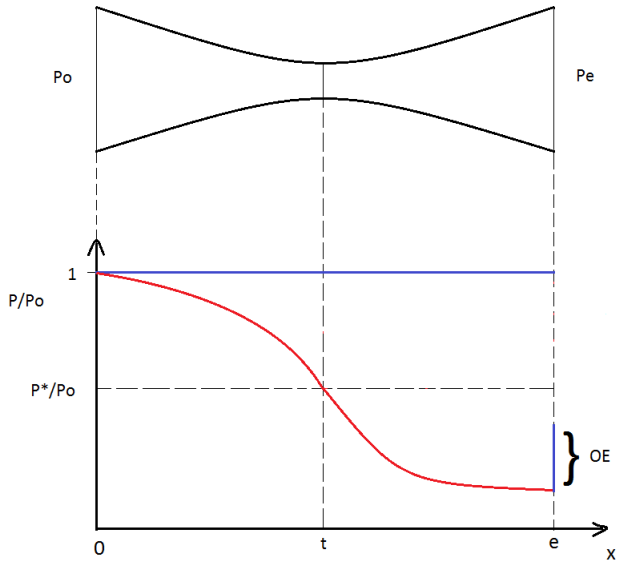

Figure 3.8: Pressure ratios along a CD nozzle considering a situation of Over Expanded Flow.

3.8.8 Underexpanded Flow

Underexpanded flow takes place when the ambient pressure is lower than what it was for the overexpanded flow, the exit pressure is considerably higher than p_b and the nozzle cannot expand the gas enough to match the ambient [14]. Contrary to the overexpanded flow, p_e needs to be lower in order to match p_b, so instead of occurring oblique shocks which increase pressure, the expansion fans will decrease the pressure [10], Figure 3.9.

There is a sequence to straight out the flow, but in an underexpanded flow it starts with an expansion fan and then an oblique shock.

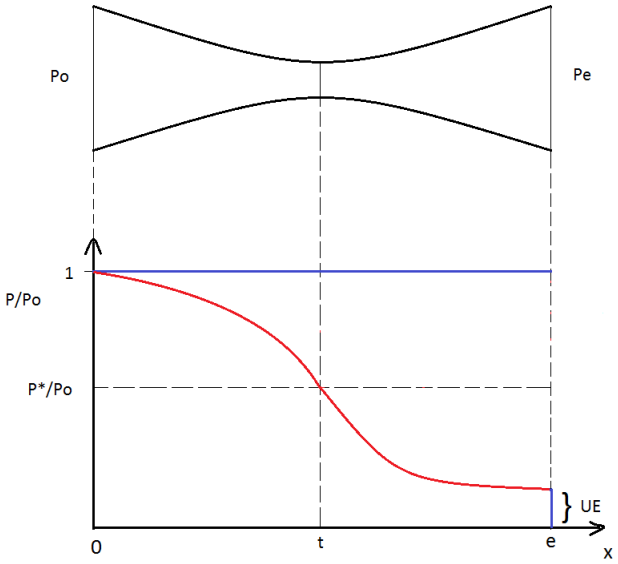

Figure 3.9: Pressure ratios along a CD nozzle considering a situation of Under Expanded Flow.

Chapter 4

Design Method

In this section the design method of a two-dimensional nozzle is presented through the method of characteristics. The procedure starts with the design of the convergent part and, depending on the exit plane radius, the same radius will be applied to the throat and thus connecting with the divergent part. The throat radius is a major factor in this work.

4.1 Method of Characteristics

The Method of Characteristics is a numerical method that has the main goal of transforming Partial Differential Equations (PDE's) into Ordinary Differential Equations (ODE's) [17] and their visual implementation with characteristic lines. The characteristic lines provide the design of shock-free supersonic nozzle considering a two-dimensional, isentropic, steady, irrotational flow [8]. This means that, the design will provide the contour of a perfectly expanded nozzle, through the solving of velocity potential. These 'lines' can be either curves or lines, the curves are composed of lines that gradually increase or decrease their angle with the direction of the flow. Along these lines, the properties of the flow are continuous but their derivatives are indeterminate. The ordinary differential equations obtained are called compatibility equations. Solving the equations in each point of the characteristic lines starting from presupposed initial conditions will generate a grid of intersecting left running and right running characteristics.

4.2 Convergent Nozzle

The design of the convergent part can be of almost any smooth contour, for example, as seen in Figure 4.1, a linear design is a good first approximation that yields decent results and achieves the sonic velocity at the throat [9].

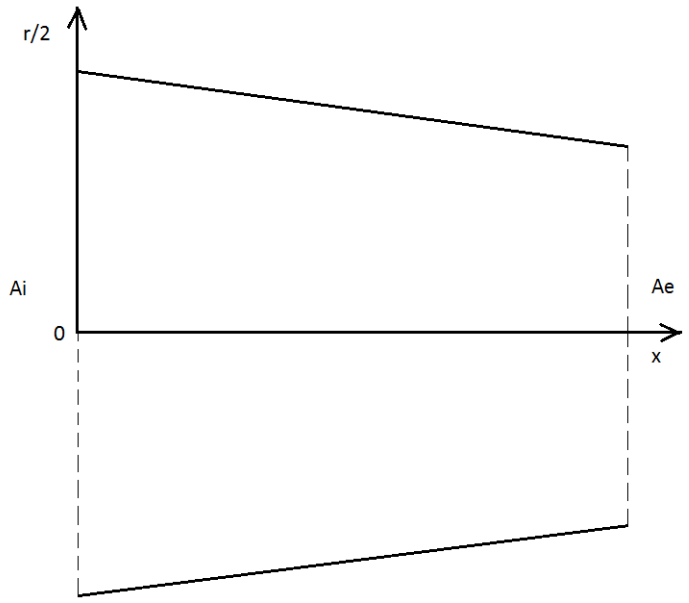

Figure 4.1: Linear design of the convergent section.

The design of the convergent part of the nozzle will start with the calculation of the radius of both the inlet (r_i) and outlet (r_e):

$$r = \sqrt{\frac{\dot{m}}{\pi \rho u}} = \sqrt{\frac{A}{\pi}} \quad (4.1)$$

Next, calculate the length of the nozzle (L) with the following equation:

$$L = \frac{r_i - r_e}{tan(\alpha)} \quad (4.2)$$

Where $11 \leq \alpha \leq 15$ [12].
The structure of a convergent nozzle is considered linear, so in order to accomplish this, the area of the nozzle decreases linearly along its length:

$$r_x = ax + b \quad (4.3)$$

$$a = \frac{r_e - r_i}{L} \qquad b = r_i$$

And the area at any point in the convergent part being:

$$A_x = \pi r_x^2 \quad (4.4)$$

The area ratio at any given station is related to the Mach number at the location by the isentropic relation:

$$\frac{A_x}{A_e} = \frac{1}{M_x}\left[\frac{2}{\gamma+1}\left(1+\frac{\gamma-1}{2}M_x^2\right)\right]^{\frac{\gamma+1}{2(\gamma-1)}} \quad (4.5)$$

The ratios of static to stagnation pressures, temperatures and densities:

$$\frac{p_x}{p_t} = \left[1+\frac{\gamma-1}{2}M_x^2\right]^{-\frac{\gamma}{\gamma-1}} \quad (4.6)$$

$$\frac{T_x}{T_t} = \left[1+\frac{\gamma-1}{2}M_x^2\right]^{-1} \quad (4.7)$$

$$\frac{\rho_x}{\rho_t} = \left[1+\frac{\gamma-1}{2}M_x^2\right]^{-\frac{1}{\gamma-1}} \quad (4.8)$$

The stagnation temperature, pressure and density are asked in the initial part of the program to the user.

$$U_x = M_x\sqrt{\gamma R T_x} \quad (4.9)$$

The velocity of the nozzle at any given point is obtained through equation 4.9.

4.3 Divergent Nozzle

On the entrance of the divergent nozzle it is assumed that the throat connects at that point and the flow is uniform, parallel and sonic. The divergent nozzle is subdivided into two zones, the expansion zone and the straightening zone. The expansion zone is curved outwards and is where the expansion of the flow, through Prandtl-Meyer expansion fans, takes place. The Mach number is increased according to maximum deflection angle, which will be explained further below, the non-simple zone of the grid of characteristics is located here. The straightening zone is where the flow is straightened and the simple zone is located, it is curved inwards.
The most important parameter of the design of this part is the exit section Mach number (M_e) which will influence the deflection angle.

4.3.1 Notions about Divergent Nozzle Design

Supersonic nozzles can be divided into two different types: gradual−expansion nozzle and minimum−length nozzle [17]. Gradual-expansion nozzles are typically used in applications

where maintaining a high quality flow at the desired exit conditions is of importance, for example with supersonic wind tunnels [18]. For other applications, such as rocket nozzles, the large weight and length penalties associated with a gradual-expansion nozzles make them unrealistic, therefore minimum-length nozzles, which use a sharp corner to provide the initial expansion, are commonly used [17].
For both gradual-expansion and minimum-length nozzles, the flow can be divided into simple and non-simple regions. A non-simple region is characterized by Mach wave reflections and intersections. In order to meet the requirements of uniform conditions at the nozzle exit, it is desirable to minimize the non-simple region as much as possible. This can be performed by designing the nozzle surface so that the Mach waves (Characteristics lines) are not produced or reflected while the flow is straightened, being the simple region.

4.3.2 Prandtl-Meyer Expansion Fan and Angle

The Prandtl-Meyer angle is the angle between the first and last Mach waves. It is useful to determine when the expansion has ended in the flow-field for a given distance away from the wall.

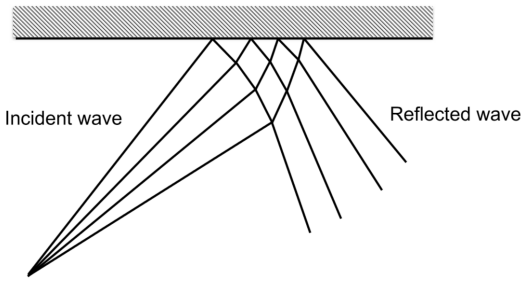

Figure 4.2: Generic expansion wave. [9]

An expansion fan, or Prandtl-Meyer wave, can be considered as a continuous sequence of infinitesimal Mach expansion waves.

$$\nu_x(M_x) = \sqrt{\frac{\gamma+1}{\gamma-1}} arctan\left(\sqrt{\frac{\gamma-1}{\gamma+1}({M_x}^2-1)}\right) - arctan\left(\sqrt{{M_x}^2-1}\right) \quad (4.10)$$

Equation 4.10 gives the Prandlt-Meyer angle at any given point of the flow, knowing the Mach number.

4.3.3 Mach Lines and Mach Angle

Mach lines, Figure 4.3, are a pair of bounding lines which separate the region of disturbed flow from the undisturbed flow, oriented at an angle μ:

$$\mu_x = sin^{-1}\left(\frac{1}{M_x}\right) \quad (4.11)$$

With respect to the direction of motion, the Mach angle is half of the angle of the Mach cone [14].

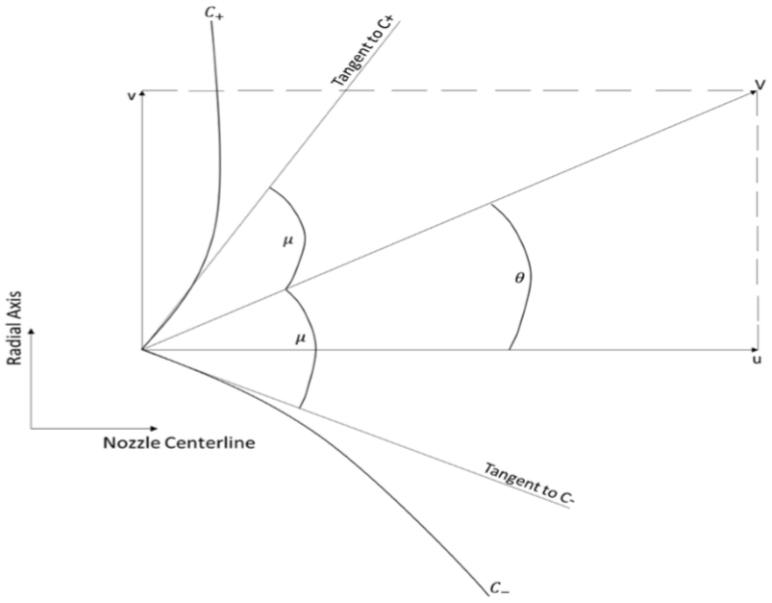

Figure 4.3: Angles of the Characteristics lines passing through a point [10].

4.3.4 Design Walkthrough

For a flow already assumed to be supersonic, inviscid, steady, two-dimensional and irrotational, the governing equation is represented below [8], being ϕ the velocity potential of the flow:

$$\left[1-\frac{1}{a^2}\left(\frac{\partial\phi}{\partial x}\right)^2\right]\frac{\partial^2\phi}{\partial x^2}+\left[1-\frac{1}{a^2}\left(\frac{\partial\phi}{\partial y}\right)^2\right]\frac{\partial^2\phi}{\partial y^2}-\frac{2}{a^2}\frac{\partial\phi}{\partial x}\frac{\partial\phi}{\partial y}\frac{\partial^2\phi}{\partial x\partial y}=0 \quad \textbf{(4.12)}$$

Knowing that $u=\partial\phi/\partial x$ and $v=\partial\phi/\partial y$ and substituting in equation (4.12):

$$\left(1-\frac{u^2}{a^2}\right)\frac{\partial^2\phi}{\partial x^2}+\left(1-\frac{v^2}{a^2}\right)\frac{\partial^2\phi}{\partial y^2}-\frac{2uv}{a^2}\frac{\partial^2\phi}{\partial x\partial y}=0 \quad \textbf{(4.13)}$$

Since the velocity potential and its derivatives are functions of x and y, can be said that:

$$d\left(\frac{\partial\phi}{\partial x}\right)=du=\frac{\partial^2\phi}{\partial x^2}dx+\frac{\partial^2\phi}{\partial x\partial y}dy \quad \textbf{(4.14)}$$

$$d\left(\frac{\partial\phi}{\partial y}\right)=dv=\frac{\partial^2\phi}{\partial x\partial y}dx+\frac{\partial^2\phi}{\partial y^2}dy \quad \textbf{(4.15)}$$

Using equations (4.13), (4.14) and (4.15), a system of equations can be built to solve this problem for $\partial^2\phi/\partial x\partial y$ employing Cramer's rule as shown in equation (4.16):

$$\frac{\partial^2\phi}{\partial x\partial y}=\frac{N}{D}=\begin{vmatrix}1-\frac{u^2}{a^2} & 0 & 1-\frac{v^2}{a^2}\\ dx & du & 0\\ 0 & dv & dy\end{vmatrix}\Bigg/\begin{vmatrix}1-\frac{u^2}{a^2} & -\frac{2uv}{a^2} & 1-\frac{v^2}{a^2}\\ dx & dy & 0\\ 0 & dx & dy\end{vmatrix} \quad \textbf{(4.16)}$$

In equation (4.16), it can be noticed that $\partial^2\phi/\partial x\partial y$ is indeterminate along the characteristic lines when both the determinant of the denominator and the numerator are equal to 0. N and D represent the determinants of the both the numerator and the denominator [8].
Setting the denominator to 0, equation (4.17), we can get the orientation of the characteristic lines and their numbers depending on the flow type (subsonic, sonic or supersonic) on each point of the flow grid.

$$\frac{\partial u}{\partial x} = \frac{\frac{2uv}{a^2} + \frac{\partial u}{\partial y} - \left(1 - \frac{v^2}{a^2}\right)\frac{\partial v}{\partial y}}{\left(1 - \frac{u^2}{a^2}\right)} \quad (4.17)$$

And, after some work, results in equation (4.18):

$$\frac{dy}{dx} = \frac{-\frac{uv}{a^2} \pm \sqrt{\left(\frac{u^2+v^2}{a^2}\right) - 1}}{\left(1 - \frac{u^2}{a^2}\right)} \quad (4.18)$$

Relation (4.18) is going to produce three cases:

1. Subsonic - $M < 1$ - This route gives imaginary roots, becoming impossible to solve, and results in elliptic PDE's;
2. Sonic - $M = 1$ - This route gives one root (one characteristic line) and results in parabolic PDE's;
3. Supersonic - $M < 1$ - This route gives two roots (two characteristic line) and results in hyperbolic PDE's.

Considering supersonic flow, one can show that:

$$u = Vcos(\theta) \quad (4.19)$$

$$v = Vcos(\theta) \quad (4.20)$$

The relationship between equations (4.18), (4.19) and (4.20), results in further simplification, which yields the following:

$$\frac{dy}{dx} = tan(\theta \pm \mu) \quad (4.21)$$

This means that at any point of inside the nozzle is the product of the crossing of two characteristic lines.
Knowing that:

$$\frac{du}{dv} = \pm\sqrt{M^2 - 1}\frac{dV}{V} \quad (4.22)$$

It can be said that:

$$d\theta = \pm\sqrt{M^2 - 1}\frac{dV}{V} \quad (4.23)$$

Which is one of the forms of the Prandtl-Meyer equation that governs the behaviour of the expansion fan. Integrating, equation (4.10) is obtained.
The compatibility equations for the characteristic lines are:

$$\theta + \nu(M) = constant = K_- \equiv C_- \quad (4.24)$$

For the right-running characteristic, the sum of those angles is constant throughout the points (intersections of lines) in those lines, shown in equation 4.24.

$$\theta - \nu(M) = constant = K_+ \equiv C_+ \quad (4.25)$$

For the left running characteristic, the subtraction of those angles is constant throughout the points (intersections of lines) in those lines, shown in equation 4.25.

4.3.5 Implementation

Figure 4.4 represents a sketch of a divergent nozzle where the contour is made with three left running characteristics and three right running characteristics. The Mach number at the throat is represented by M_t and the exit Mach number is represented by M_e. Point A is where the sharp turn takes place and point a and C are present in the same characteristic line. The angle θ is equal to zero degrees when the point is in the x axis or when the slope of the contour is parallel to the x axis.

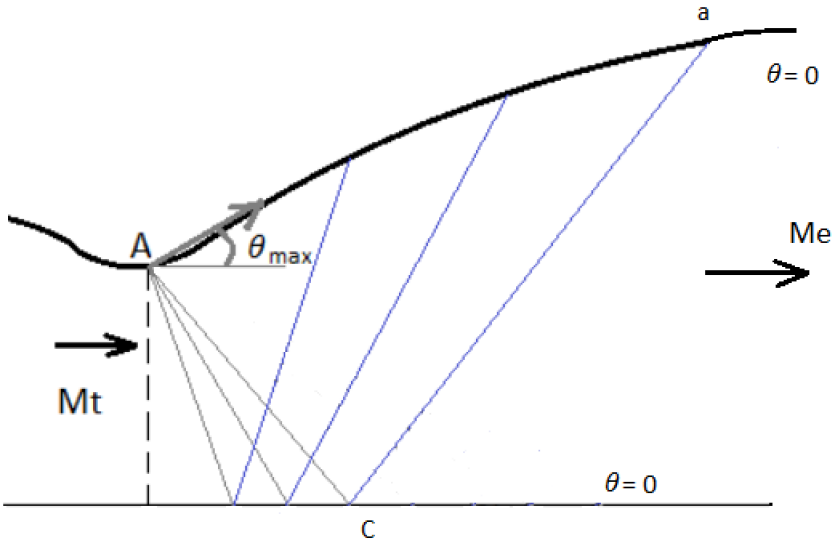

Figure 4.4: Initial example of 3 characteristic lines.

Along characteristic $C - a$ (left characteristic), using the compatibility equations:

$$\theta_C = \theta_a = 0$$
$$\theta_C - \nu_C = \theta_a - \nu_a \iff$$
$$\iff \nu_C = \nu_a = \nu(M_e)$$

On $A - C$ (right characteristic):

$$\theta_A = \nu_A = \theta_{max}$$
$$\theta_A + \nu_A = \theta_C + \nu_C \iff$$
$$\iff \theta_{max} = \frac{\nu(M_e)}{2} \qquad (4.26)$$

With relation (4.26) one can see that the maximum θ angle is solely a function of the exit Mach number. The maximum θ angle is independent of the number of characteristic lines, but a higher number of characteristic lines increases accuracy in relation to the reality of the contour.

4.3.5.1 Internal Points

Figure 4.5 illustrates three points, two known points, 1 and 2, and an unknown point, 3. Through point 1 a right-running characteristic passes [19], and through point 2, a left-running characteristic passes [19], intersecting at point 3.

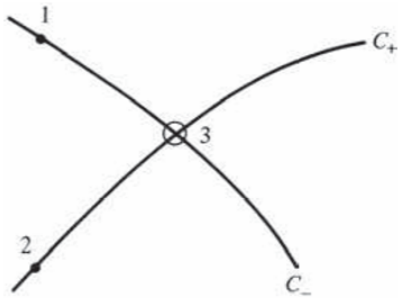

Figure 4.5: Example of the intersection of two characteristics inside the nozzle from two known points [8].

Since the value of a characteristic remains constant throughout, by definition, on point 3, $(K_+)_3 = (K_+)_2$ and $(K_-)_3 = (K_-)_1$, as seen in equations (4.27) and (4.28). These constants are called Riemann invariants [8].

$$(K_+)_3 = (K_+)_2 = \theta_2 - \nu_2 \quad (4.27)$$

$$(K_-)_3 = (K_-)_1 = \theta_1 + \nu_1 \quad (4.28)$$

From the compatibility equations, the following is obtained for point 3:

$$(K_+)_3 = \theta_3 - \nu_3 \quad (4.29)$$

$$(K_-)_3 = \theta_3 + \nu_3 \quad (4.30)$$

Combining equations (4.27), (4.28), (4.29) and (4.30), the values of both θ_3 and ν_3 are obtained via equations (4.31) and (4.32):

$$\theta_3 = \frac{1}{2}[(K_-)_1 + (K_+)_2] \quad (4.31)$$

$$\nu_3 = \frac{1}{2}[(K_-)_1 - (K_+)_2] \quad (4.32)$$

As explained in (4.1), the characteristic lines between points are, by convenience, assumed as straight lines, each having specific slopes [17]. In this case, the segments between points 1 and 3, 2 and 3 are straight lines. The slope for the left-running characteristic is obtained applying equation (4.33) and the slope for the right-running characteristic is obtained applying equation (4.34):

$$m_1 = \tan\left[\frac{1}{2}(\theta_1 + \theta_3) - \frac{1}{2}(\mu_1 + \mu_3)\right] \quad (4.33)$$

$$m_2 = \tan\left[\frac{1}{2}(\theta_2 + \theta_3) + \frac{1}{2}(\mu_2 + \mu_3)\right] \quad (4.34)$$

The location of the point 3, in coordinates, is obtained with the intersection of the characteristics crossing that point, which is shown with equations (4.35), (4.36) and (4.37):

$$x_3 = \frac{y_1 - y_2 + m_2 x_2 - m_1 x_1}{m_2 - m_1} \quad (4.35)$$

$$y_3 = y_1 + m_1(x_3 - x_1) \quad (4.36)$$

$$y_3 = y_2 + m_2(x_3 - x_2) \quad (4.37)$$

4.3.5.2 Wall Points

Figure 4.6 shows the first left-running characteristic that creates the contour of the wall, passing through points 7 and 8.

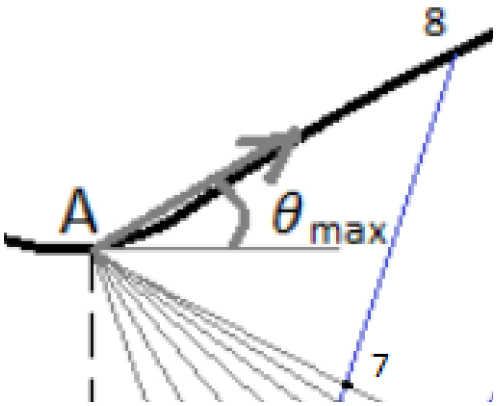

Figure 4.6: Example of a wall point.

The location of point 8 is found with the intersection of the line passing through point A with the angle θ_{max} and the left running characteristic passing through point 8. Since the Riemann invariant of a characteristic is constant throughout, $(K_+)_7 = (K_+)_8$ as shown in equation (4.38) and (4.39):

$$(K_+)_7 = (K_+)_8 = \theta_7 - \nu_7 \quad (4.38)$$

$$(K_+)_8 = \theta_8 - \nu_8 \quad (4.39)$$

The slope of the characteristic is given by equation (4.40):

$$m_{78} = \tan\left[\frac{1}{2}(\theta_7 + \theta_8) + \frac{1}{2}(\mu_7 + \mu_8)\right] \quad (4.40)$$

Point A is assumed to be known, and the only unknown variable is ν_8 due to θ_8 being equal to θ_{max}.

$$\nu_8 = \nu_7 + \theta_8 - \theta_7 \quad (4.41)$$

4.3.5.3 Regions of influence and dependence of the points

In steady supersonic flow, the disturbances caused in a single point are not felt completely around that point, they are only felt in a particular region downstream of that point. In figure 4.7, it can be seen two different regions related to the point A, the region of dependence and the region of influence. Both regions are located inside the left running and right running characteristic lines. The region of dependence is the area upstream of the point, and the properties of that point are conditioned by it. The region of influence is located downstream of point A and the properties on that area are conditioned by the properties of point A [20].

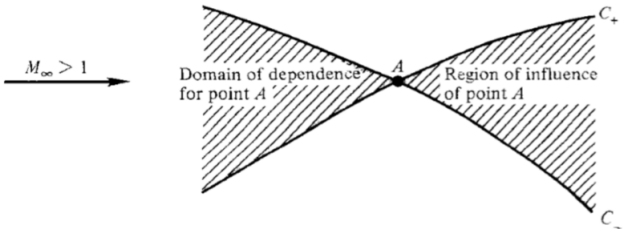

Figure 4.7: Regions of dependence and influence of point A.

4.4 Coding Steps and Walkthrough

The design of the contour and the graphics, presented in 5 chapter, were made solely resorting to MATLAB.
Applying the concepts demonstrated in the previous sections, the code was built having in mind the overall speed to obtain the results, this meaning that, the efficiency was the most crucial aspect. The work was divided into three main parts: the input box, the convergent section and the divergent section.
In the following sections it is explained step by step how every part of the code works, starting from the inputs, the ones needed for each section, then the main body where the calculations are implemented and how the loops work, and finally, the plots that show the results. The formulas used are explained in both sections 4.2 and 4.3.
The main objective is to show to the user the contour, the various properties and ratios along the nozzle. Those properties and ratios being: Mach number, temperature, static to stagnation temperature, density, static to stagnation density, pressure and static to stagnation pressure.

4.4.1 Input Dialog Box

The input dialog box is the main part of the code, where both the convergent section function and the divergent section function are called.
The initiation of the input dialog box is a choice menu, where the program asks the user the type of operation and from the box that shows up, there are two options: Thrust or Mass flow, this is just a means to ease the user work while using this program, since the Thrust is a function of the Mass flow.
On the code, the boxes are inside an ‘If’ statement, where the Thrust box is the first choice, and the Mass flow box is inside the ‘else’ statement. Inside each of those choices, the commands used were, by order:

1. prompt - Statement to insert the names of each input box inside the dialog box;
2. dlg title - Inserts the title of the dialog box;
3. num lines - Number of lines that each input box has, in this case it is just one;
4. def - Defines the number of input boxes, in this case there are 9 inputs, each of them is represented inside the def statement with double apostrophe;
5. inputdlg - The actual command that groups the last four statements and shapes the box.

The number of inputs is nine because when the user, for example, chooses the Thrust option, the Mass flow is considered as zero automatically.
After the statements were written, each of the inputs are assigned to different variables and need to be transformed from a string to a number that MATLAB can read. For this effect, it was used the command 'str2double'.
Subsequently, the functions of the convergent section and the divergent section are called, and the variables introduced to obtain the results.

4.4.2 Convergent Section

The convergent section is the simplest sector of the nozzle because, as said before, it is assumed that it has a linear shape.

4.4.2.1 Inputs

The inputs were divided into three different categories: inlet inputs, outlet inputs and overall inputs. In this section, the inlet is the actual inlet of the nozzle, the outlet is the region near the throat and the overall inputs are related to the entire flow and do not change throughout.
The inlet inputs used are: the inlet pressure, it is the static pressure of the flow that comes from the combustion chamber, the inlet temperature, it is the static temperature of the flow that comes from the combustion chamber and the inlet velocity of the flow.
The outlet inputs used are: the outlet pressure, it is the static pressure of the flow that arrives at the throat, the outlet temperature, it is the static temperature of the flow that arrives at the throat and the outlet velocity of the flow. The overall inputs used are: the mass flow or specific thrust, the specific heat ratio, the real gas constant and the stagnation temperature.
There are two inputs that are not requested to the user, being those the number of stations that the convergent section divides that defines the contour to avoid the excessive division of such a simple design

4.4.2.2 Main Body

The main body of the convergent section code starts with the calculations of some basic aspects of the nozzle, the inlet and outlet densities, areas, radius and Mach numbers. It is also determined the appropriate length (L) of the convergent part.
The contour design, has referred in (4.2), is a simple linear shape. The two variable used are:

1. x - Represents each station, starts at zero;
2. r - Represents the radius on each station throughout the nozzle.

The different variables that need to be obtain through the next series of loops made use of the 'for' statement running from station one to the number of stations desired. The variable x increments its value L/St each loop.
Following the radius, the area and the Mach number are determined. The area is obtained through the circle area formula and then the area ratios are calculated.
The Mach number is iterated based on a solver, where the Mach number is the variable to be found and setting the function of the Area-Mach relation to zero. Using the MATLAB function 'fzero' the roots of the function for each area ratio is found and only the subsonic root is allowed to demonstrated the results in the Mach number distribution plot.

Since most of the next properties and their respective ratios are functions of the Mach number, the order of the code until the plots is made according to the order in [12].

4.4.2.3 Plots

The plots are divided into four separate figures, each of one of them bearing two graphics where subplots are used. Those subplots represent the variables calculate in each station.

4.4.3 Divergent Section

In the divergent section the contour is not linear and each of the final points of the characteristic lines give the shape to the wall. The plot of the characteristic lines and the contour is made along the code and not in three lines, unlike the plots for the Mach distribution temperature, pressure, density and their respective ratios along the nozzle.
The main objective of this section is to obtain a contour similar to the one shown on Figure 4.8, that shows a divergent shape with seven characteristic lines, but in the code, the number of characteristic lines depends on the maximum angle θ at point A, that in turn depends on the exit Mach number.

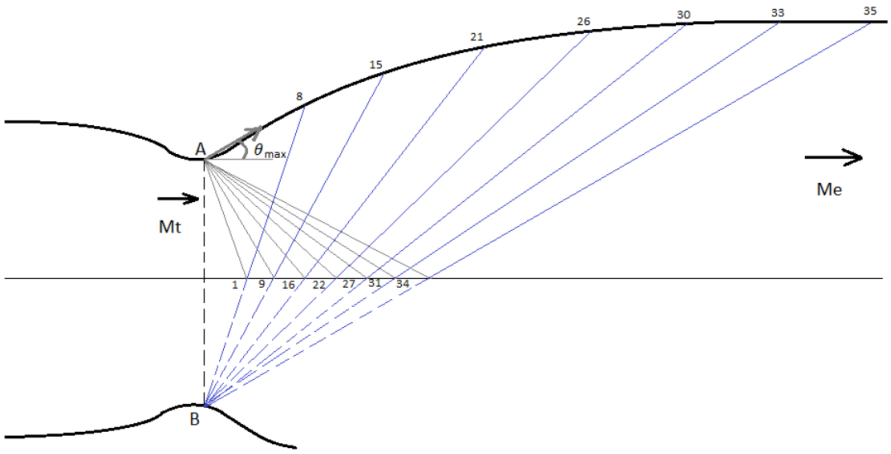

Figure 4.8: Schematic of the characteristic lines with seven wall points.

4.4.3.1 Inputs

The number of inputs requested to the user for the divergent section are fewer than the ones requested for the convergent section due to the existing thermodynamic relations between the variables and having less freedom of choice to change those variables.
The inputs required are: the chamber pressure, the chamber temperature, the mass flow or thrust, the altitude, the specific gas constant, the real gas constant and the throat radius, that in this case is the inlet radius..

4.4.3.2 Main Body

The main body of the divergent design, taken from NASA website [21], starts with the calculation of the ambient pressure, which uses the altitude to determine it.
With the ambient pressure, it can be discovered some variables at the throat: the temperature, the pressure and the velocity.

After the throat variables, the exit variables are determined: the exit velocity, temperature and the local speed of sound.
Knowing the exit velocity and the local speed of sound, the exit Mach number can be computed, which was the main objective to be found until now.
To begin the actual design of the contour, the Prandtl-Meyer function is introduced using a solver in which the Mach number is the variable, it is called later in the code. MATLAB can not express some function using degrees, so two lines were introduced to convert degrees into radians, and radians to degrees.
Plugin the exit Mach number on the Prandtl-Meyer function, the maximum θ angle is obtained, which in turn is going to be divided n divisions of θ. The number of divisions are equivalent to the total of loops inside a 'for' statement where the Mach number, the axis points, the right-running and left-runnings slopes are computed. Those characteristic are plotted and a grid is formed. The grid is not completed here.
The wall points are divided into three sections: the first wall point, the middle points and the last point, due to the first point being almost perpendicular to the center line and the last point needed to be parallel to the center line. Simple trigonometrical solution are used to find the first and last wall points, the middle points are looped using a 'for' statement with incremental θ angles.
The distributions of temperature, density, pressure, velocity and respective ratios are computed using the same functions as in the convergent section, introducing the supersonic Mach number obtained. The number of stations is correspondent to the length of the Mach number vector.

4.4.3.3 Plots

The plots are divided into four separate figures, each of one of them bearing two graphics where subplots are used. Those subplots represent the variables calculate in each station.

Chapter 5

Results

This chapter explains the results obtained via the design method presented in chapter 4 and what happens when the code is ran. It is divided into three different parts: the Input Dialog Box Mechanics, the Case Studies and the Obstacles that still remain in the code.
In the Input Dialog Box Mechanics it is described what the code shows to the user when it initiates, and the two routes that can be chosen, the Thrust route and the Mass Flow route.
The Case Studies presents three different cases and their respective designs. The variables are changed to simulate distinct situations and how the contour of the nozzle changes as well as the graphics that display the Mach number, temperature, density, pressure and their ratios.
The Obstacles that still remain in the code, as the name states, demonstrate certain aspects of the code that can be improved with future works.
The design of the contour and the graphics, presented in this chapter, were solely made resorting to MATLAB software.

5.1 Input Dialog Box Mechanics

As the code is started, the box shown in Figure 5.1 is presented to the user. It is asks the user the preferential type of operation, one where the thrust is part of the variables or another that the mass flow is the one of the variables. After the selection of the operation another box for inputs appears.

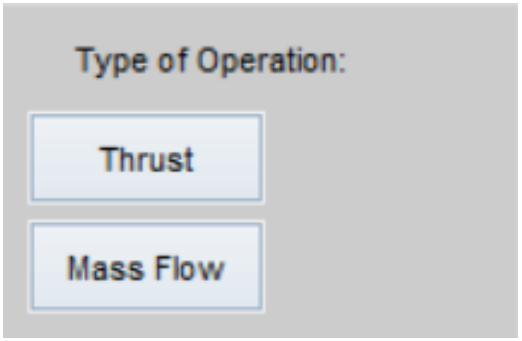

Figure 5.1: Box that initializes the code and select the type of operation.

5.1.1 Thrust Route

If the Thrust option was selected, the box shown in Figure 5.2 appears to the user. The input box asks for the following variables: total temperature, flow velocity at the inlet, convergent contour inclination ($11 < \theta < 15$), chamber temperature (inlet temperature), chamber pressure (inlet pressure), thrust desired, cruise altitude, specific heat ratio (normally for air $\gamma = 1.4$), real gas constant, flow velocity right before the throat, temperature right before the throat (outlet temperature) and pressure right before the throat (outlet pressure), all on the SI units.

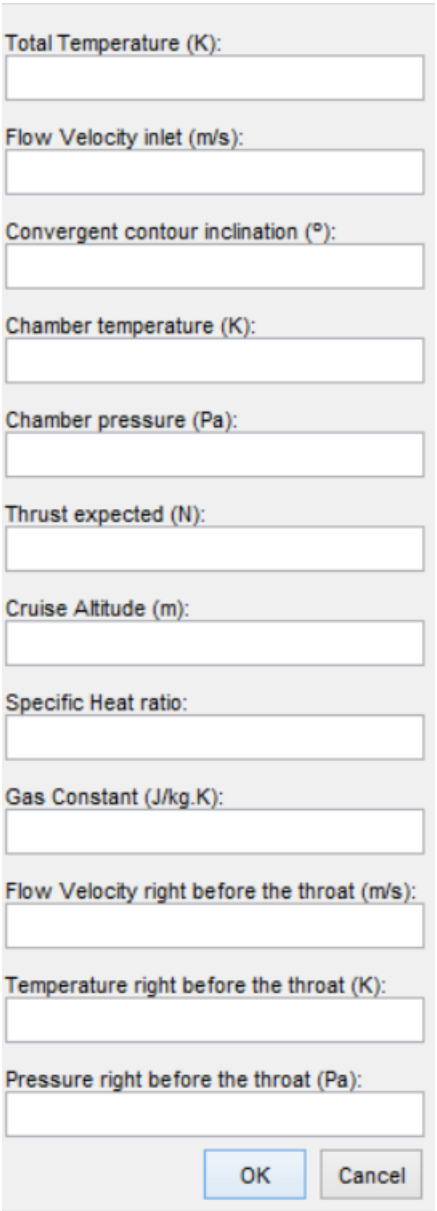

Figure 5.2: Input dialog box after selecting the Thrust option.

5.1.2 Mass Flow Route

If the Mass flow option was selected, the box shown in Figure 5.2 appears to the user. The input box asks for the following variables: total temperature, flow velocity at the inlet, convergent contour inclination ($11 < \theta < 15$), chamber temperature (inlet temperature), chamber pressure (inlet pressure), mass flow desired, cruise altitude, specific heat ratio (normally for air $\gamma = 1.4$), real gas constant, flow velocity right before the throat, temperature right before the throat (outlet temperature) and pressure right before the throat (outlet pressure), all on the SI units.

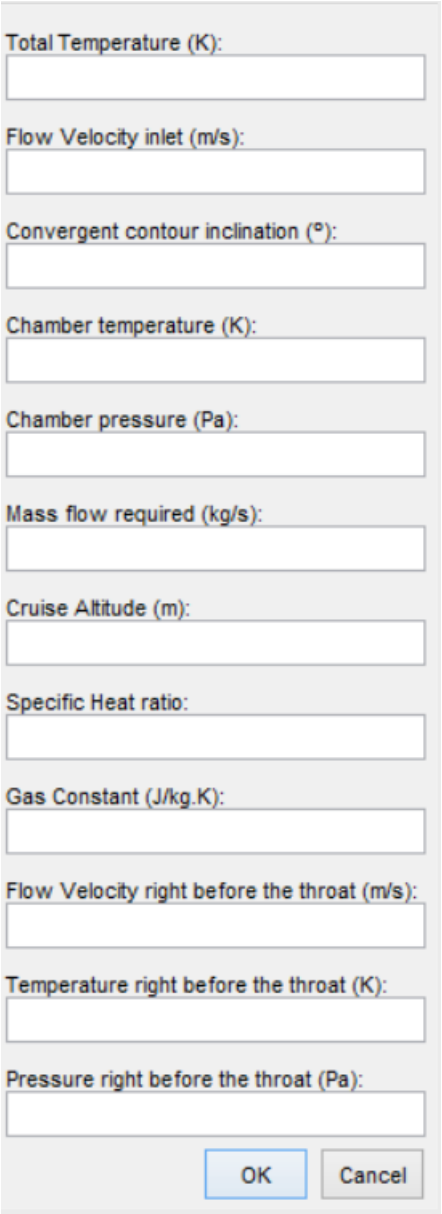

Figure 5.3: Input dialog box after selecting the Mass Flow option.

5.2 Case Studies

The case studies shows three cases where the mass flow is changed to understand the effect that the mass flow has on the parameters of the flow inside the nozzle.
Each of the cases is divided in the results for the two sections: convergent section and the divergent section.
The values of the parameters that do not change, used for the three cases, are as follows:

Table 5.1: Fixed Parameters

Total Temperature (K)	755
Flow Velocity inlet (m/s)	131.56
Convergent contour inclination (°)	11
Chamber temperature (K)	747.5
Chamber pressure (Pa)	2270000
Cruise Altitude (m)	1000
Specific Hear Ratio	1.4
Gas Constant (J/kg.K)	287.05
Flow Velocity right before the throat (m/s)	497.61
Temperature right before the throat (K)	647.1
Pressure right before the throat (Pa)	1180400

The parameters are computed for each stations, the convergent section has fourteen stations while the divergent section has 44 stations. The values of the inlet are iterated from the values given in the table 5.1. The stage 15 represents the throat. Since the Mach number does not achieve the value required for choked flow, the throat radius was computed assuming the flow is choked [12]. On the C Annex, the parameters at each station can be found on tables for each specific case.

5.2.1 Case 1

In the first case, the mass flow is set at $80\ \frac{kg}{s}$, it is expected that the inlet and outlet areas to be bigger than for the second and third cases.

5.2.1.1 Convergent Section

As observed in Figure 5.4, the shape of the convergent section, in this case, is a linear contour. It has an inlet radius of $0.135m$ and an outlet radius of $0.093m$. At the inlet, station 1, the Mach number has a value of 0.26, and the outlet, station 14, the Mach number has a value of 0.73 which is already a transonic regime.

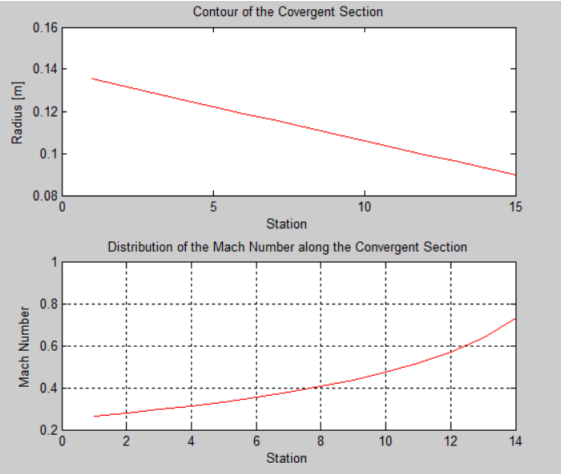

Figure 5.4: Contour and Mach Number distribution along the Convergent section.

One of the most important parameters that needs to be verified is the static to total pressure ratio. As explained in chapter 3.8, observing Figure 5.5, the static to total pressure ratio decreases in a negative parabolic way, starting from ratio at the inlet with 0.95 and at the outlet with 0.7, it is assumed that at the throat the pressure ratio reaches a value of, around, 0.52. The static pressure also decreases in a parabolic way, having at the inlet a value of $2047000Pa$ and an outlet value of $1507400Pa$.

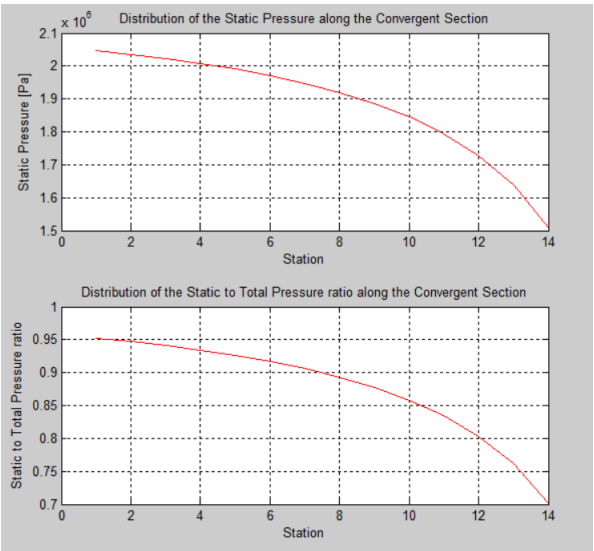

Figure 5.5: Distribution of the Static Pressure and Static to Total pressure ratio along the Convergent section.

The static temperature and static to total temperature ratio are shown in Figure 5.6, it depicts a parabolic curve for both parameters, the inlet values are $744.49K$ and 0.98, and the outlet values are $682.16K$ and 0.9, respectively.

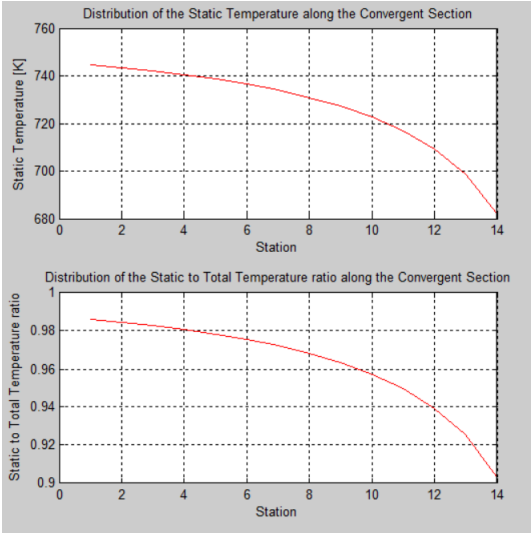

Figure 5.6: Distribution of the Static Temperature and Static to Total Temperature ratio along the Convergent section.

In Figure 5.7, it can be noticed that the static density and the static to total density ratio of the flow decreases in a parabolic way, the inlet values are $9.57\frac{kg}{m^3}$ and 0.96, and the outlet values are $7.69\frac{kg}{m^3}$ and 0.776, respectively.

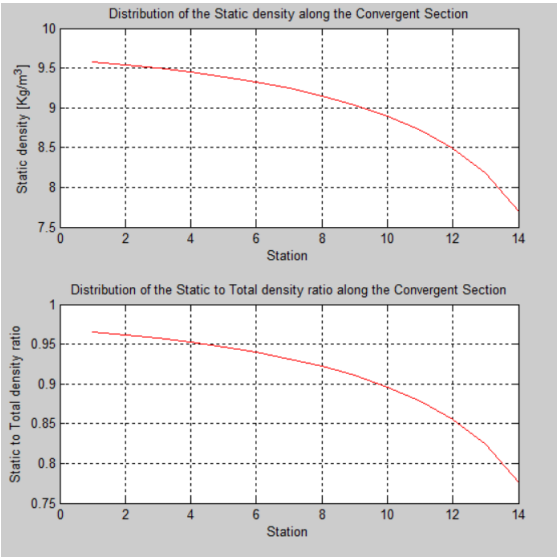

Figure 5.7: Distribution of the Static density and Static to Total density ratio along the Convergent section.

5.2.1.2 Divergent Section

As observed in Figure 5.8, the shape of the divergent section, in this case, is a curved contour. The connection of last point of the characteristics forms the contour, and the mass flows plays a big role in the shape of the contour. It has a throat radius of $0.0897m$ and an outlet radius of $0.128m$. The length of the divergent section is $0.207m$.

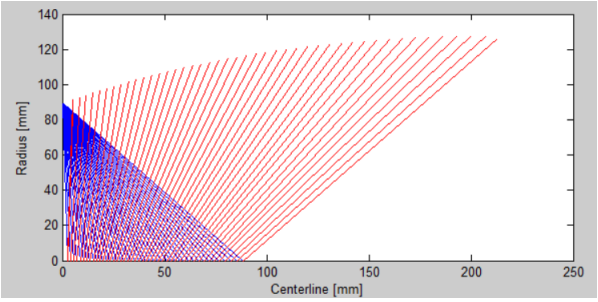

Figure 5.8: Contour of the Divergent section.

At the inlet, station 1, the Mach number has a value of 1.11, and at the outlet, station 44, the Mach number has a value of 2.74 which is the exit velocity, the nozzle achieves supersonic flow, as seen in Figure 5.9.

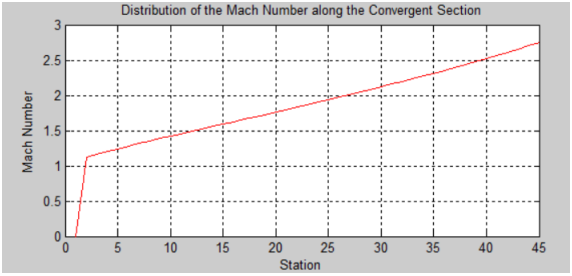

Figure 5.9: Mach Number distribution along the Divergent section.

As in the convergent section, the pressure is the main parameter. Figure 5.10 shows the static pressure and the static to total pressure ratio. Both of the parameters decrease in a upwards parabolic way, as explained in chapter 3.8. The static to total pressure ratio starts at the throat with a value of 0.46 and at the outlet a value of 0.04, and the static pressure starts at the inlet with a value of $1427800Pa$ and an outlet value of $216490Pa$. The flow of the nozzle is overexpanded, for the an optimal expansion the static pressure should have the value of around $89874Pa$ at an altitude of $1000m$.

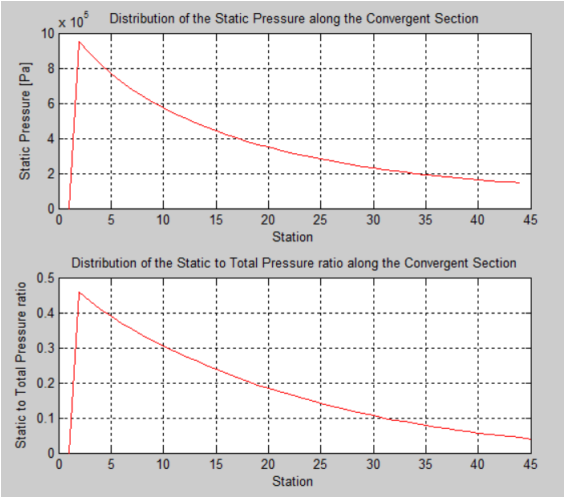

Figure 5.10: Distribution of the Static Pressure and Static to Total pressure ratio along the Divergent section.

Observing Figure 5.11, the static temperature and static to total temperature ratio decrease in a linear way. At the throat the static temperature has a value of $604.71K$ and at the outlet a value of $307.12K$. The static to total temperature ratio has a value of, at the throat, of 0.8 and at the outlet a value of 0.4.

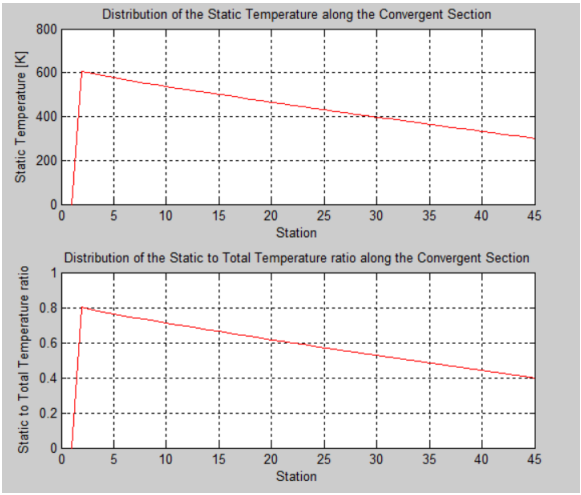

Figure 5.11: Distribution of the Static Temperature and Static to Total Temperature ratio along the Divergent section.

In Figure 5.12, it can be noticed that the static density and the static to total density ratio of the flow decreases in a upwards parabolic way, the inlet values are $5.48\frac{kg}{m^3}$ and 0.57, and the outlet values are $1.63\frac{kg}{m^3}$ and 0.1, respectively.

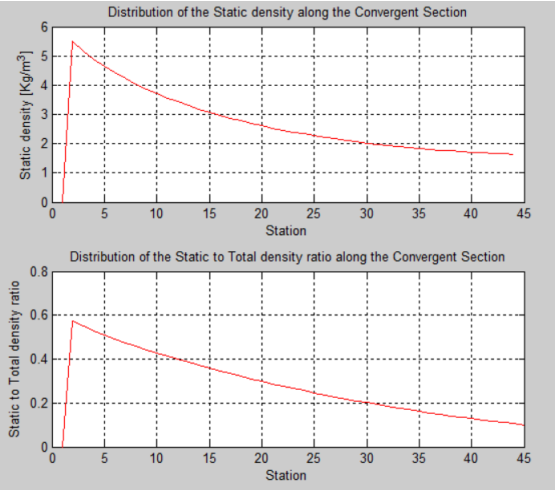

Figure 5.12: Distribution of the Static density and Static to Total density ratio along the Divergent section.

5.2.2 Case 2

In the second case, the mass flow is set at $60\ \frac{kg}{s}$, it is expected that the inlet and outlet areas have values between those of the first and third case.

5.2.2.1 Convergent Section

Observing Figure 5.13, the shape of the convergent section, in this case, is a linear contour. It has an inlet radius of $0.117m$ and an outlet radius of $0.08m$. At the inlet, station 1, the Mach number has a value of 0.26, and the outlet, station 14, the Mach number has a value of 0.73 which is already a transonic regime.

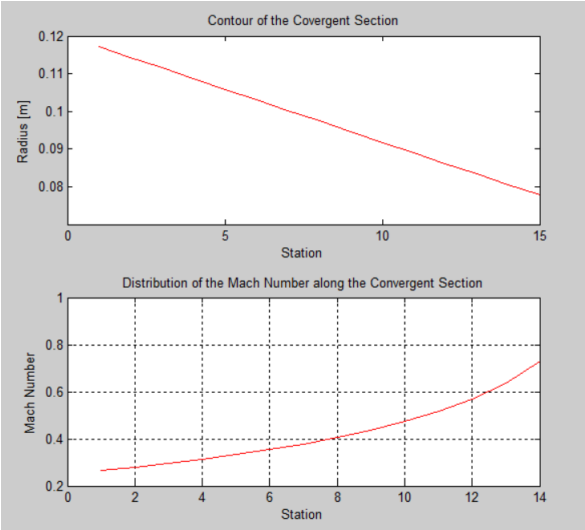

Figure 5.13: Contour and Mach Number distribution along the Convergent section.

One of the most important parameters that needs to be verified is the static to total pressure ratio. As explained in chapter 3.8, observing Figure 5.14, the static to total pressure ratio decreases in a negative parabolic way, starting from ratio at the inlet with 0.95 and at the outlet with 0.7, it is assumed that at the throat the pressure ratio reaches a value of, around, 0.52.

The static pressure also decreases in a parabolic way, having at the inlet a value of $2047000Pa$ and an outlet value of $1507400Pa$.

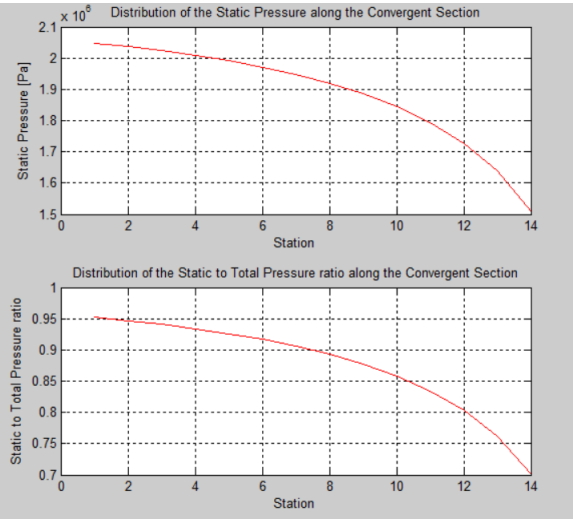

Figure 5.14: Distribution of the Static Pressure and Static to Total pressure ratio along the Convergent section.

The static temperature and static to total temperature ratio are shown in Figure 5.15, it depicts a parabolic curve for both parameters, the inlet values are $744.49K$ and 0.98, and the outlet values are $682.16K$ and 0.9, respectively.

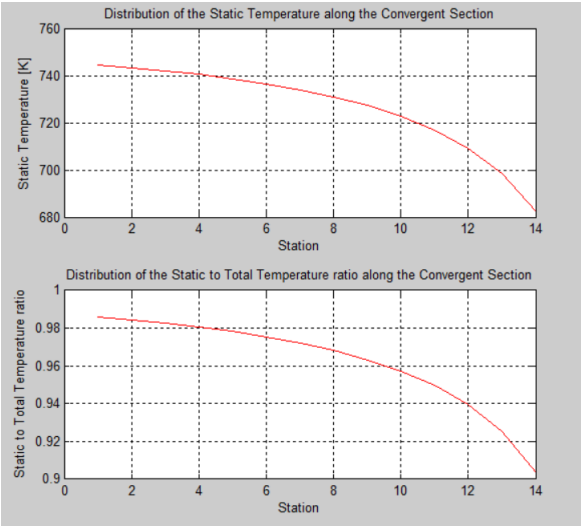

Figure 5.15: Distribution of the Static Temperature and Static to Total Temperature ratio along the Convergent section.

In Figure 5.16, it can be noticed that the static density and the static to total density ratio of the flow decreases in a parabolic way, the inlet values are $9.57\frac{kg}{m^3}$ and 0.96, and the outlet values are $7.69\frac{kg}{m^3}$ and 0.776, respectively.

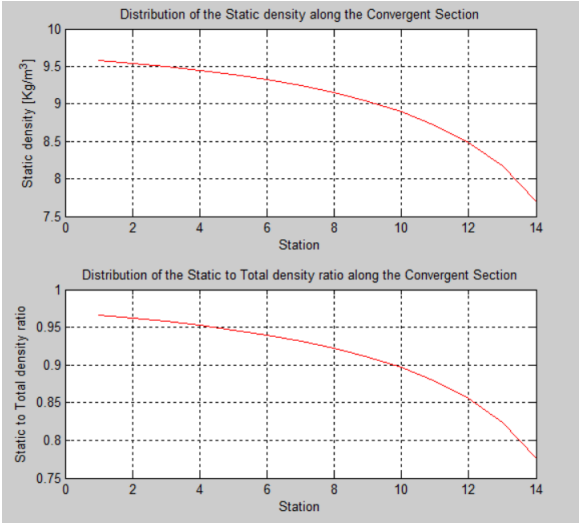

Figure 5.16: Distribution of the Static density and Static to Total density ratio along the Convergent section.

5.2.2.2 Divergent Section

Observing Figure 5.17, the shape of the divergent section, in this case, is a curved contour. The connection of last point of the characteristics forms the contour. It has an inlet radius of $0.0777m$ and an outlet radius of $0.110m$. The length of the divergent section is $0.179m$.

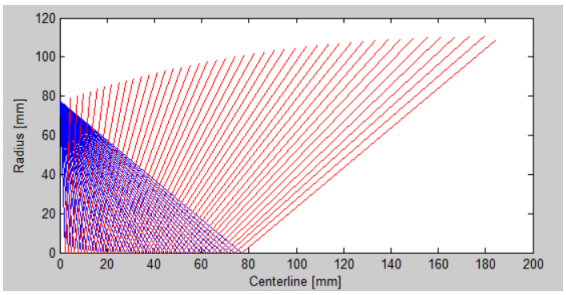

Figure 5.17: Contour of the Divergent section.

At the inlet, station 1, the Mach number has a value of 1.11, and the outlet, station 44, the Mach number has a value of 2.74 which is the exit velocity, the nozzle achieves supersonic flow, as seen in Figure 5.18.

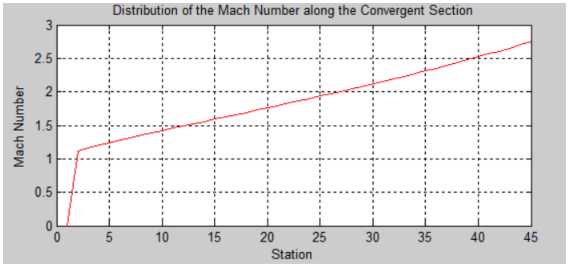

Figure 5.18: Mach Number distribution along the Divergent section.

As in the convergent section, the pressure is the main parameter. Figure 5.19 shows the static pressure and the static to total pressure ratio. Both of the parameters decrease in a upwards

parabolic way, as explained in chapter 3.8. The static to total pressure ratio starts at the throat with a value of 0.46 and at the outlet a value of 0.04, and the static pressure starts at the inlet with a value of $1427800Pa$ and an outlet value of $216490Pa$. The flow of the nozzle is overexpanded, for the an optimal expansion the static pressure should have the value of around $89874Pa$ at an altitude of $1000m$.

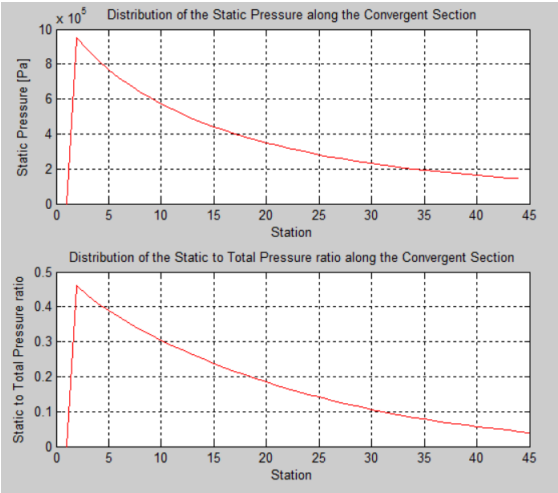

Figure 5.19: Distribution of the Static Pressure and Static to Total pressure ratio along the Divergent section.

Observing Figure 5.20, the static temperature and static to total temperature ratio decrease in a linear way. At the throat the static temperature has a value of $604.71K$ and at the outlet a value of $307.12K$. The static to total temperature ratio has a value of, at the throat, of 0.8 and at the outlet a value of 0.4.

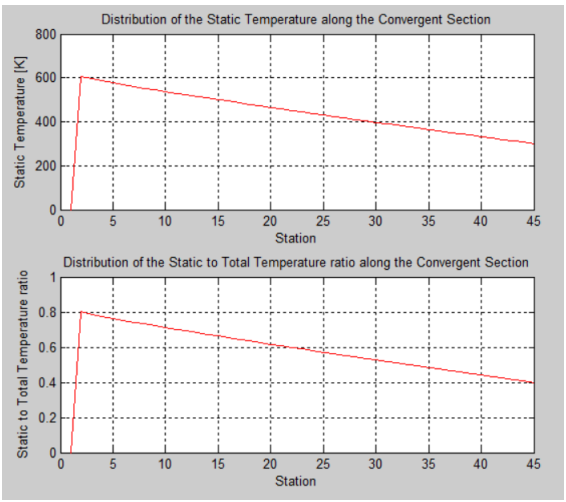

Figure 5.20: Distribution of the Static Temperature and Static to Total Temperature ratio along the Divergent section.

In Figure 5.21, it can be noticed that the static density and the static to total density ratio of the flow decreases in a parabolic way, the inlet values are $9.57\frac{kg}{m^3}$ and 0.96, and the outlet values are $7.69\frac{kg}{m^3}$ and 0.776, respectively.

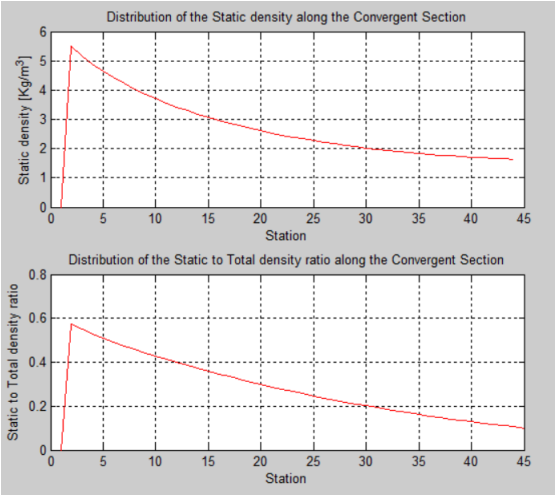

Figure 5.21: Distribution of the Static density and Static to Total density ratio along the Divergent section.

5.2.3 Case 3

In the third case, the mass flow is set at $40\ \frac{kg}{s}$, it is expected that the inlet and outlet areas to be the smaller values between the three cases.

5.2.3.1 Convergent Section

The shape of the convergent section, in this case, is a linear contour, as seen in Figure 5.22. It has an inlet radius of $0.0.095m$ and an outlet radius of $0.065m$. At the inlet, station 1, the Mach number has a value of 0.26, and the outlet, station 14, the Mach number has a value of 0.73 which is already a transonic regime.

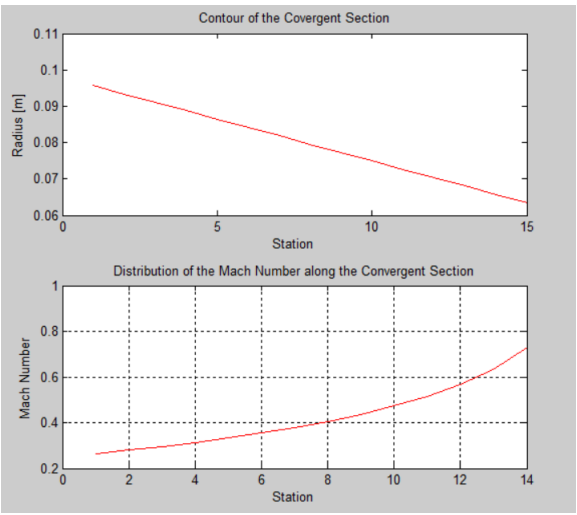

Figure 5.22: Contour and Mach Number distribution along the Convergent section.

One of the most important parameters that needs to be verified is the static to total pressure ratio. As explained in chapter 3.8, observing Figure 5.23, the static to total pressure ratio decreases in a negative parabolic way, starting from ratio at the inlet with 0.95 and at the outlet with 0.7, it is assumed that at the throat the pressure ratio reaches a value of, around, 0.52.

The static pressure also decreases in a parabolic way, having at the inlet a value of $2047000Pa$ and an outlet value of $1507400Pa$.

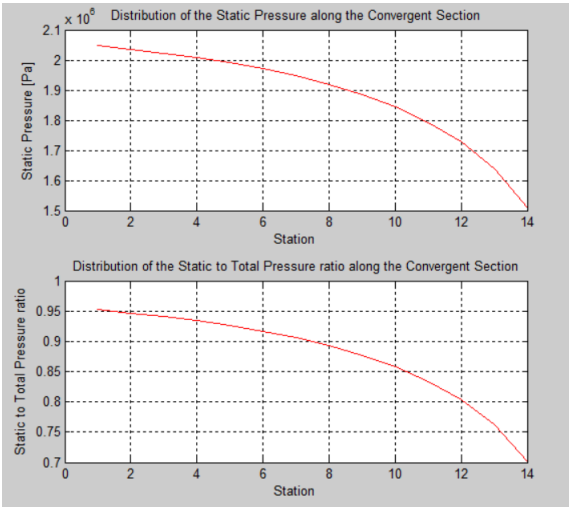

Figure 5.23: Distribution of the Static Pressure and Static to Total pressure ratio along the Convergent section.

The static temperature and static to total temperature ratio are shown in Figure 5.24, it depicts a parabolic curve for both parameters, the inlet values are $744.49K$ and 0.98, and the outlet values are $682.16K$ and 0.9, respectively.

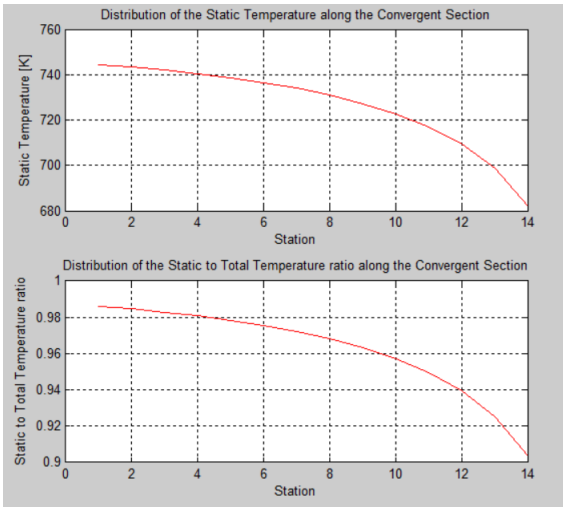

Figure 5.24: Distribution of the Static Temperature and Static to Total Temperature ratio along the Convergent section.

In Figure 5.25, it can be noticed that the static density and the static to total density ratio of the flow decreases in a parabolic way, the inlet values are $9.57\frac{kg}{m^3}$ and 0.96, and the outlet values are $7.69\frac{kg}{m^3}$ and 0.776, respectively.

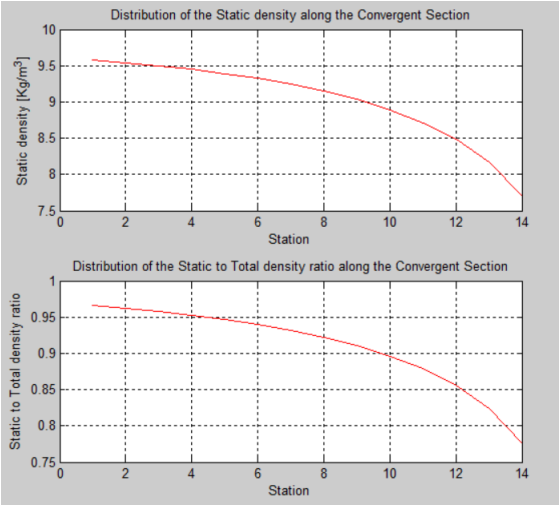

Figure 5.25: Distribution of the Static density and Static to Total density ratio along the Convergent section.

5.2.3.2 Divergent Section

Observing Figure 5.26, the shape of the divergent section, in this case, is a curved contour. The connection of last point of the characteristics forms the contour. It has an inlet radius of $0.0635m$ and an outlet radius of $0.090m$. The length of the divergent section is $0.146m$.

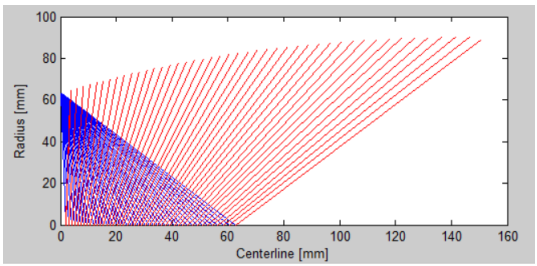

Figure 5.26: Contour of the Divergent section.

At the inlet, station 1, the Mach number has a value of 1.11, and the outlet, station 44, the Mach number has a value of 2.74 which is the exit velocity, the nozzle achieves supersonic flow, as seen in Figure 5.27.

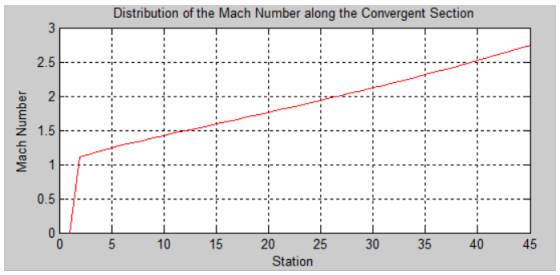

Figure 5.27: Mach Number distribution along the Divergent section.

As in the convergent section, the pressure is the main parameter. Figure 5.28 shows the static pressure and the static to total pressure ratio. Both of the parameters decrease in a upwards parabolic way, as explained in chapter 3.8. The static to total pressure ratio starts at the throat

with a value of 0.46 and at the outlet a value of 0.04, and the static pressure starts at the inlet with a value of $1427800Pa$ and an outlet value of $216490Pa$. The flow of the nozzle is overexpanded, for the an optimal expansion the static pressure should have the value of around $89874Pa$ at an altitude of $1000m$.

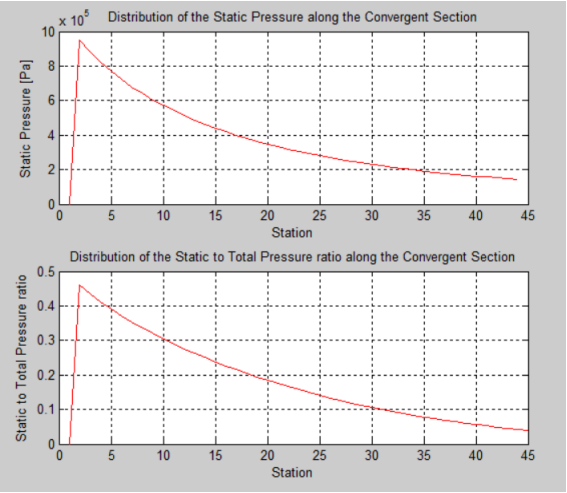

Figure 5.28: Distribution of the Static Pressure and Static to Total pressure ratio along the Divergent section.

Observing Figure 5.29, the static temperature and static to total temperature ratio decrease in a linear way. At the throat the static temperature has a value of $604.71K$ and at the outlet a value of $307.12K$. The static to total temperature ratio has a value of, at the throat, of 0.8 and at the outlet a value of 0.4.

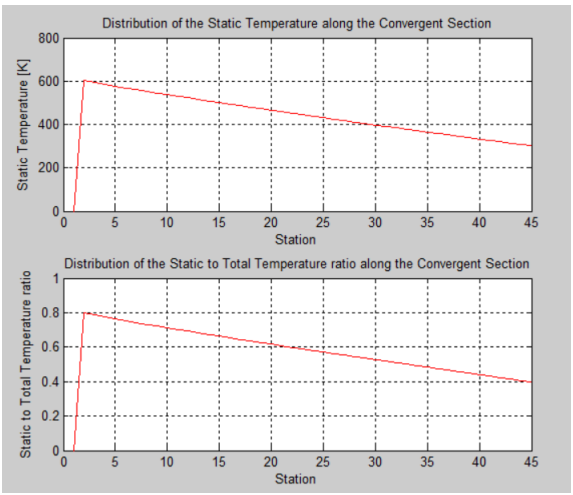

Figure 5.29: Distribution of the Static Temperature and Static to Total Temperature ratio along the Divergent section.

In Figure 5.30, it can be noticed that the static density and the static to total density ratio of the flow decreases in a parabolic way, the inlet values are $9.57\frac{kg}{m^3}$ and 0.96, and the outlet values are $7.69\frac{kg}{m^3}$ and 0.776, respectively.

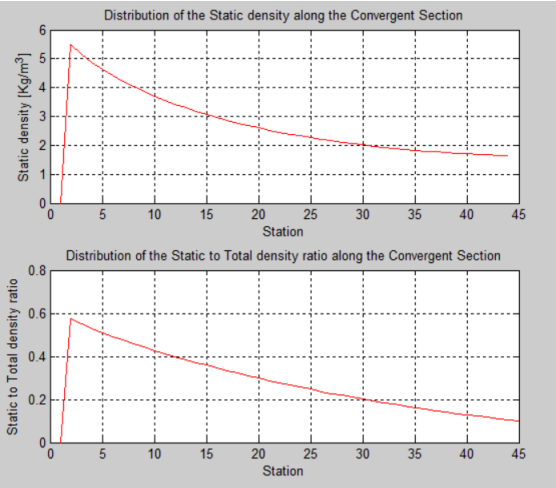

Figure 5.30: Distribution of the Static density and Static to Total density ratio along the Divergent section.

Chapter 6

Conclusion

The continue growth of propulsion technology, accompanied by the evolution of aircrafts, demands highly complex coding to provide conceptual designs with the least amount of independent variables.
The focus was the implementation of a code that asked the user the design parameters and the return of the nozzle, including the throat parameters.
This dissertation employs a method of the design of a supersonic CD nozzle, that eases the work of the user of running each part of the code individually. The user can simply write the parameters in the input box and the design is made automatically as well and the export of the parameters, in each stage, to the excel file selected.
The application of the Method of Characteristic was the center-part of the this work and enabled the design of the divergent section, which is the most complex due to the expansion fans forms on the corners of the throat, it was confirmed that the process described in this work applying the Method of Characteristic produces a design of supersonic nozzle.
With the limited time available, the results provided some conclusion, even with several assumption, for instance, assuming isentropic quasi-one dimensional flow for the calculations. The mass flow is an important parameter but, as can be observed in the chapter 5, it does not affect the other important parameters, for example, the static pressure and the static to total pressure distributions, only influencing the shape of the convergent and divergent section. It can also be observed that increasing the mass flow, the nozzle inlet, throat, exit area and length increase. The results obtained provided some corroboration to what was described in chapter 3. In the three cases, the pressure distributions along the nozzle follow the path described in chapter 3, on the convergent section there is a downwards parabolic curve approximates the values of choked flow at the throat, and on the divergent section the pressure ratio distribution are represented with a upwards parabolic curve tending to values of optimal expanded flow. In this case, the flow was overexpanded since the pressure ratio in the outlet, on all three cases, was higher than the one required for optimal expanded flow.
In conclusion, even though the main goal of achieving a perfectly expanded flow, the design of both the convergent part and the divergent part was achieve and can provide other students the steeping stone and the knowledge necessary to achieve better results.

6.1 Future Work

The contents of this work resulted in an experimental method of the applications of the Method of characteristics and represent the beginning of the development of the design of a CD nozzle. As the propulsion technology advances, the variable geometry nozzle are becoming more important. The implementation of a variable geometry throat in this work would really complement the code and approximate it with the reality.
As for the throat values, it would be recommended that a choked flow can be achieved, this can be done easily, finding an approach that the Mach number at the throat reaches 1.

To enhance the code approximation the reality an optimization code should be implemented to execute faster, utilize memory efficiently and have an overall better performance.
In regard to the flow in the divergent section, in this dissertation, an overexpanded flow was attained. The flow inside a nozzle should be perfectly expanded, the implementation of this aspect avoids the occurrences of oblique shocks outside the nozzle.

Bibliography

[1] (2018) a319 convergent nozzle. xv, 4

[2] (2014) F-18 nozzles. [Online]. Available: https://photography-on-the.net/forum/showthread.php?t=1361018 xv, 5

[3] (2009) F-22 non-axisymetric nozzle. [Online]. Available: http://www.f-16.net/forum/viewtopic.php?t=11981 xv, 6

[4] T. MIZUKAKI. (2016) Visualization of stagnation point inside the closed wake of a 20 percent - truncated plug nozzle at starting process. [Online]. Available: https://www.sciencedirect.com/science/article/pii/S1270963815300043 xv, 6

[5] (2016) Ejector nozzle. [Online]. Available: https://aeronotes.weebly.com/ejector-nozzle.html xv, 7

[6] C. Hunge. (2015) Su-35 iris nozzle. [Online]. Available: https://www.pinterest.pt/pin/695946948640250575/ xv, 7

[7] AgentJayZ. (2011) Afterburner spark test. xv, 8

[8] J. D. Anderson, *Fundamentals of Aerodynamics*. McGraw-Hill Education, 2017. [Online]. Available: https://www.amazon.com/Fundamentals-Aerodynamics-John-Anderson-Jr/dp/1259129918 xv, 10, 11, 12, 14, 17, 18, 19, 20, 29, 33, 34, 36

[9] O. B. George P. Sutton, *Rocket Propulsion Elements*. John Wiley and Sons, Inc., 8th edition. xv, xvii, 12, 13, 16, 21, 30, 32, 89

[10] D. Y. K. Uyeki, "A design method for a supersonic axisymmetric nozzle for use in wind tunnel facilities," no. 2, pp. 1–92, 2018. xv, 26, 33

[11] N. A. S. Command, *Aircraft Engines and Systems*. Chief of Naval Air Training, 2001. 3

[12] A. F. El-Sayed, *Aircraft Propulsion and Gas Turbine Engines, Second Edition*. CRC Press, 2017. [Online]. Available: https://www.crcpress.com/Aircraft-Propulsion-and-Gas-Turbine-Engines/El-Sayed/p/book/9781466595163 4, 7, 8, 10, 18, 30, 41, 46

[13] R. R. C. David M. Straight, "Thrust performance of a variable-geometry, nonaxisymmetric, two-dimensional, convergent-divergent exhaust nozzle on a turbojet engine at altitude," no. 5, pp. 1–40, 1983. 5

[14] P. M. Sforza, *Theory of Aerospace Propulsion*. Elsevier, 2016. [Online]. Available: https://www.elsevier.com/books/theory-of-aerospace-propulsion/sforza/978-0-12-809326-9 5, 6, 7, 12, 14, 20, 21, 22, 23, 24, 26, 32

[15] M. Onofri, "Plug nozzles: Summary of flow features and engine performance," no. 4, pp. 1–26, 2006. 6

[16] O. Singh, *Applied Thermodynamics*. New Age International. 10, 12

[17] M. S. D. C. Md Akhtar Khan, Sanjay Kumar Sardiwal, "Design of a supersonic nozzle using method of characteristics," no. 1, pp. 1–7, 2013. 29, 31, 32, 37

[18] H. C. G. S. K. S. T. S. Parv Khurana, Saurabh Jindal, "Supersonic nozzle design using method of characteristics," no. 3, pp. 1–8, 2017. 32

[19] G. Dimitriadis, *Aerodthermodynamics of High Speed Flow*. University of Liège. 36

[20] J. D. Anderson, *Modern Compressible Flow*. McGraw-Hill Education, 2003. [Online]. Available: https://www.amazon.com/Modern-Compressible-Flow-Historical-Perspective/dp/0072424435 38

[21] N. Hall. (2015) Earth atmosphere model. [Online]. Available: https://www.grc.nasa.gov/WWW/K-12/airplane/atmosmet.html 41

Appendices

A Basic Definitions

A.1 Force

A force is an interaction between objects or substances, with mass, that causes a change in their motion. Considering that the mass of the body is constant the acceleration, is directly proportional to the force applied on it. The body undergoing study can be at rest or already in motion.
The forces are normally represented by a vector with direction and magnitude and by the letter F in the SI unit system measured with Newtons (N).
Specifying for thermodynamics, a thermodynamic force is a measurement of energy orientation within a system when it is not in thermodynamic equilibrium.

A.2 Pressure

Since this thesis revolves around fluids, the pressures influencing the environment in study are used to ease the understanding behind the mechanics of the flow, instead of the forces only.
Pressure is the ratio of force applied perpendicular to the surface of an object or substance per unit area of that surface where the force is allocated. The SI unit for pressure is the Pascal (Pa), which is Newton per square meter and the letter that represent it is P. Other units can also be used for pressure and are rather common, for example, in terms of the standard atmospheric pressure (atm) or involving mercury (torr).
The pressures present in this work are mainly the absolute pressure, static pressure and dynamic pressure. The static pressure is the potential energy of the fluid molecules at rest, the dynamic is the kinetic energy of the molecules of the fluid in motion and the absolute is the sum of the two previous pressures.

A.3 Drag

Drag is the force opposing the motion of a substance or object. Following the drag equation for a fluid, one can observe that the velocity of the flow is directly proportional to the drag, as the velocity increases the drag increases and the same happens with density. Specifically, for this thesis, the main form of drag used is caused by the inertia of the fluid is called pressure drag.

A.4 Temperature

One definition of temperature is the assessment of the kinetic energy of the molecules within a system. With this assessment one can determine the direction of heat flow. Considering two systems, the heat flow will always go from the one with the highest temperature to the one with the lowest temperature and it will stop when the thermodynamic equilibrium is reached.
The SI unit for pressure is the Kelvin (K), which is equal to the temperature in Celsius plus 273.15.

A.5 System

The system is a particular region of the universe which is undergoing study, its limits are covered by the boundary, an imaginary division, and beyond the boundaries there are the surroundings.

A thermodynamic system is a system in which the thermodynamic properties are being studied. Exchanges within a system, as heat and work, are of interest when comparing with a real life situation, since a thermodynamic system is an approximation of a real one. There are three types of systems: open system, closed system and isolated system.

A.5.1 Isolated System

Isolated systems do not allow exchanges of energy and mass with the surroundings, maintaining the energy and mass constant. An isolated system possesses a boundary that keeps its mass constant, it's perfectly insulated or adiabatic avoiding transfers of energy in the form of heat and it is rigid thus there are no transfers of energy in the form of work.

A.5.2 Closed System

Closed systems allow the transfer of energy but there is an absence of transfers of mass. The mass within a closed system is constant while the energy can release or absorbed through heat and work on the boundary.

A.5.3 Open System

Open systems allow the transfer of both energy and mass with the surroundings. An open system cannot achieve an equilibrium state.

A.6 Intensive Properties

Intensive properties of the flow do not depend on the system size or its mass. Some of these properties are the pressure, temperature, density and the specific heats.

A.7 Extensive Properties

Extensive properties, opposed to the intensive ones, depend on the system size or its mass, for instance, if the amount of matter in the system doubles, the extensive properties double in value. The ratio between two extensive properties is an intensive property. Some of these properties are the mass, volume, weight and the internal energy.

A.8 State

State indicates the precise condition of the system. This condition is discovered when a series of properties are known and have value, the number of properties needed to define a system depends on its complexity. The same happens with a thermodynamic system, to discover the state there is a need to know the specific value of a series of measurable thermodynamic properties that are sufficient to determine the remaining unknown state variables.

B Code

B.1 Input Box

```
close all
clear all
clc

%% Inputs Menus

choice = menu('Type of Operation:','Thrust','Mass Flow');

if choice == 1

prompt = {'Total Temperature (K):','Flow Velocity inlet (m/s):',
'Convergent contour inclination (º): ','Chamber temperature (K):',
'Chamber pressure (Pa):','Thrust expected (N):',
'Cruise Altitude (m):','Specific Heat ratio:',
'Gas Constant (J/kg.K):','Flow Velocity right before the throat (m/s):',
'Temperature right before the throat (K):',
'Pressure right before the throat (Pa):'};
dlg_title = 'Enter details of operation:';
num_lines = 1;
def = {'','','','','','','','','','','',''};
box1 = inputdlg(prompt,dlg_title,num_lines,def);

T0 = str2double(box1{1});
Vchamber = str2double(box1{2});
theta = str2double(box1{3});
Tchamber = str2double(box1{4});
Pchamber = str2double(box1{5});
FT = str2double(box1{6});
Alt = str2double(box1{7});
g = str2double(box1{8});
R = str2double(box1{9});
Vtr = str2double(box1{10});
Ttr = str2double(box1{11});
Ptr = str2double(box1{12});
m_dot = 0;

else

prompt = {'Total Temperature (K):','Flow Velocity inlet (m/s):',
'Convergent contour inclination (º): ','Chamber temperature (K):',
'Chamber pressure (Pa):','Mass flow required (kg/s):',
```

```
'Cruise Altitude (m):','Specific Heat ratio:','Gas Constant (J/kg.K):',
'Flow Velocity right before the throat (m/s):',
'Temperature right before the throat (K):',
'Pressure right before the throat (Pa):'};
dlg_title = 'Enter details of operation:';
num_lines = 1;
def = {'','','','','','','','','','','',''};
box1 = inputdlg(prompt,dlg_title,num_lines,def);

T0 = str2double(box1{1});
Vchamber = str2double(box1{2});
theta = str2double(box1{3});
Tchamber = str2double(box1{4});
Pchamber = str2double(box1{5});
m_dot = str2double(box1{6});
Alt = str2double(box1{7});
g = str2double(box1{8});
R = str2double(box1{9});
Vtr = str2double(box1{10});
Ttr = str2double(box1{11});
Ptr = str2double(box1{12});
FT = 0;

end

%% Function Calls

re = Convergent(theta,m_dot,g,R,T0,FT,Pchamber,Tchamber,Vchamber,Ptr,Ttr,Vtr);

TR = re*1000;

Divergent(Pchamber,Tchamber,FT,m_dot,Alt,g,R,TR);
```

B.2 Convergent Section

```
function re = Convergent(theta1,mdot1,g1,R1,To1,FT1,Pi1,Ti1,Vi1,Pe1,Te1,Ve1)

%% Inputs

theta = theta1; % 11          % degrees
m_dot = mdot1;  % 65          % kg/s
g = g1;         %1.4
R = R1;         %287.05       % J/kg.K
To = To1;       %1000         % Kelvin
FT = FT1;       %0            % Newtons
```

```
%Inlet

Pi = Pi1;          %63230;      % Pascal
Ti = Ti1;          %747.5;      % Kelvin
Vi = Vi1;          %131.56;     % m/s

%Outlet

Pe = Pe1;          %36130;      % Pascal
Te = Te1;          %647.1;      % Kelvin
Ve = Ve1;          %497.617;    % m/s

%% Calculations Inlet and Outlet

St = 14;           % Number of station
gm1 = g-1;
gp1 = g+1;

%Densities

rho_i = Pi/(R*Ti); % kg/m^3
rho_e = Pe/(R*Te); % kg/m^3

%Inlet and Outlet Areas and radius

Ai = m_dot/(rho_i*Vi); % m^2
Ae = m_dot/(rho_e*Ve); % m^2

ri = sqrt(m_dot/(pi*rho_i*Vi)); % m
re = sqrt(m_dot/(pi*rho_e*Ve)); % m

%Length of the nozzle

RTOD = 180/pi; % Rad to Degrees
DTOR = pi/180; % Degrees to Rad

thetaRAD = theta*DTOR;
L = (ri - re)/tan(thetaRAD); % m

%Local Mach

Mi = Vi/(sqrt(g*R*Ti));
Me = Ve/(sqrt(g*R*Te));

%Thrust and Mass flow transformation
```

```
if m_dot==0
    m_dot=FT/Ve;
elseif FT==0
    FT = m_dot/Ve;
end

%% Contour Design

r = [];
Xaxys = [];
a = (re - ri)/L;
b = ri;
x = 0;
Xaxys = 0;

for i = 1:St

    r(i) = a*x+b;
    x = x + L/(St);

end

for i = 2:St

    Xaxys(i) = Xaxys(i-1) + L/(St);

end

Xaxys(St+1) = L;
r(St+1) = re;

%% Mach Distribution

M = [];
A = [];
ARatio = [];
%M(1) = Mi;
%A(1) = Ai;
%ARatio(1) = (A(1))/Ae;

errTol = 1e-4;  % Error tolerance

verboseBisection   = 0;       % Flags for printing iterations to screen
verboseIncremental = 0;       % Flags for printing iterations to screen

for i = 1:St
```

```
A(i) = (pi*r(i)^2); %(square meters)

ARatio(i) = (A(i))/Ae;

% Set up the solver
problem.objective = @(M) (1/M^2)*(((2+gm1*M^2)/gp1)^(gp1/gm1))-(ARatio(i))^2;
% Objective function
problem.solver    = 'fzero'                % Find the zero
problem.options   = optimset(@fzero);      % Default options

% Solve subsonic root
problem.x0 = [1e-6 1];                     % Subsonic solver bounds
Msub(i)    = fzero(problem);               % Solve for subsonic M

end

%A(St+1) = Ae;
%Msub(St+1) = (Ae/A(St+1))*((2/(g+1))*(1+((g-1)/2)*(Me)^2))^((g+1)/(2*(g-1)));

%% Temperature Distribution

T = [];
TTo = [];
%T(1) = Ti;

for i = 1:St

    TTo(i) = (1+((g-1)/2)*(Msub(i))^2)^(-1);

end

%TTo(St+1) = (1+((g-1)/2)*(Msub(St+1))^2)^(-1);

for i = 1:St

    T(i) = To*(1+((g-1)/2)*(Msub(i))^2)^(-1);

end

%T(St+1) = To*(1+((g-1)/2)*(Msub(St+1))^2)^(-1);

%% Velocity Distribution

V = [];
V(1) = Vi;

for i = 1:St
```

```
    V(i) = Msub(i)*sqrt(g*R*T(i));

end

%V(St+1) = Msub(St+1)*sqrt(g*R*T(St+1));

%% Density Distribution

rho = [];
rhorhoo = [];
rho(1) = rho_i;

for i = 1:St

    rhorhoo(i) = (1+((g-1)/2)*(Msub(i))^2)^((-1)/(g-1));

end

for i = 1:St

    rho(i) = m_dot/(V(i)*A(i));

end

%rhorhoo(St+1) = (1+((g-1)/2)*(Msub(St+1))^2)^((-1)/(g-1));
%rho(St+1) = m_dot/(V(St+1)*A(St+1));

%% Pressure Distribution

P = [];
PPo = [];
P(1) = Pi;

for i = 1:St

    PPo(i) = (1+((g-1)/2)*(Msub(i))^2)^((-g)/(g-1));

end

for i = 1:St

    P(i) = rho(i)*R*T(i);

end

%PPo(St+1) = (1+((g-1)/2)*(Msub(St+1))^2)^((-g)/(g-1));
```

```
%P(St+1) = rho(St+1)*R*T(St+1);

xlswrite('NozzleExcel.xlsx',transpose(r),'Convergent','A1:A20');
xlswrite('NozzleExcel.xlsx',transpose(Xaxys),'Convergent','B1:B20');
xlswrite('NozzleExcel.xlsx',transpose(A),'Convergent','C1:C20');
xlswrite('NozzleExcel.xlsx',transpose(ARatio),'Convergent','D1:D20');
xlswrite('NozzleExcel.xlsx',transpose(Msub),'Convergent','E1:E20');
xlswrite('NozzleExcel.xlsx',transpose(T),'Convergent','F1:F20');
xlswrite('NozzleExcel.xlsx',transpose(TTo),'Convergent','G1:G20');
xlswrite('NozzleExcel.xlsx',transpose(V),'Convergent','H1:H20');
xlswrite('NozzleExcel.xlsx',transpose(rhorhoo),'Convergent','I1:I20');
xlswrite('NozzleExcel.xlsx',transpose(rho),'Convergent','J1:J20');
xlswrite('NozzleExcel.xlsx',transpose(PPo),'Convergent','K1:K20');
xlswrite('NozzleExcel.xlsx',transpose(P),'Convergent','L1:L20');


%% Plots

figure(1)
subplot(2,1,1)
plot(r,'r')
xlabel('Station')
ylabel('Radius [m]')
title('Contour of the Covergent Section')

subplot(2,1,2)
plot(Msub,'r')
grid on
xlabel('Station')
ylabel('Mach Number')
title('Distribution of the Mach Number along the Convergent Section')

%%
figure(2)
subplot(2,1,1)
plot(T,'r')
grid on
xlabel('Station')
ylabel('Static Temperature [K]')
title('Distribution of the Static Temperature along the Convergent Section')

subplot(2,1,2)
plot(TTo,'r')
grid on
xlabel('Station')
ylabel('Static to Total Temperature ratio')
title('Distribution of the Static to Total Temperature
```

```
ratio along the Convergent Section')

%%
figure(3)
subplot(2,1,1)
plot(rho,'r')
grid on
xlabel('Station')
ylabel('Static density [Kg/m^3]')
title('Distribution of the Static density along the Convergent Section')

subplot(2,1,2)
plot(rhorhoo,'r')
grid on
xlabel('Station')
ylabel('Static to Total density ratio')
title('Distribution of the Static to Total
density ratio along the Convergent Section')

%%
figure(4)
subplot(2,1,1)
plot(P,'r')
grid on
xlabel('Station')
ylabel('Static Pressure [Pa]')
title('Distribution of the Static Pressure along the Convergent Section')

subplot(2,1,2)
plot(PPo,'r')
grid on
xlabel('Station')
ylabel('Static to Total Pressure ratio')
title('Distribution of the Static to Total
Pressure ratio along the Convergent Section')

end
```

B.3 Divergent Section

```
function Divergent(Pchamb,Tchamb,FT1,mdot1,Alt1,g1,R1,TR1)

%Inputs
p_1 = Pchamb;       %Chamber pressure
T_1 = Tchamb;        %Chamber temperature
```

```
FT = FT1;           %Desired Thrust (Option 1)
m_dot = mdot1;      %Desired Mass Flow (Option 2)
ALT = Alt1;         %Altitude
g = g1;             %Specific heat constant
R = R1;             %Gas Constant
TR = TR1;           %Throat radius

%%
if (11000<ALT) && (ALT<25000)

    Tout = -56.46; %C
    p_o = 1000*(22.65*exp(1.73-0.000157*ALT));

elseif ALT>=25000

    Tout = -131.21 + 0.00299*ALT ;
    p_o = 1000*(2.488*((Tout+273.1)/216.6)^-11.388);

else

    Tout = 15.04 - 0.00649*ALT;
    p_o = 1000*(101.29*((Tout+273.1)/288.08)^5.256);

end

%%
PR = p_o/p_1;
PR2 = (p_o/p_1)^((g-1)/g);

TT = (2*g*R*T_1)/(g-1);
p_t = ((2/(g+1))^(g/(g-1)))*2.068;

v_t = sqrt((2*g*R*T_1)/(g+1));
v_e = sqrt(TT*(1-PR2));

if m_dot==0

    m_dot=FT/v_e;

elseif FT==0

    FT = m_dot/v_e;

end

T_e = T_1*(p_o/p_1)^((g-1)/g);
a_e = sqrt(g*R*T_e);
```

```
Me = v_e/a_e;

% MOC
RTOD = 180/pi;
DTOR = pi/180;
P = []; %x axis points

%%
A = sqrt((g+1)/(g-1));
B = (g-1)/(g+1);
v_PM = @(x) A*atan(sqrt(B*(x^2-1))) - atan(sqrt(x^2-1));


%%
T_max = 0.5*v_PM(Me)*RTOD;
DT = (90-T_max) - fix(90-T_max); % Retira parte
decimal do valor total do angulo
T(1) = DT*DTOR; %Primeiro valor do array é a
parte decimal do angulo
n = T_max*2;

for m = 2:n+1

    T(m) = (DT + (m-1))*DTOR;
    x_int = [1 1.01*Me];
    func = @(x) T(m) - v_PM(x);
    M(m) = fzero(func,x_int);
    P(m) = 0 + TR*tan(T(m));
    RR(m) = -TR/P(m);
    LR(m) = tan(T(m)+asin(1/M(m)));
    SL(m) = -RR(m);

end

%%
P(1) = [];
l = length(P);

figure(5)

for j = 1:l
    P1 = [0 TR];
    P2 = [P(j) 0];
    plot(P2,P1,'b')
    hold on
    xlabel('Centerline [mm]')
```

```
    ylabel('Radius [mm]')
end

hold on;

LR(1) = []; RR(1) = [];
SL(1) = [];
F = RR(m-1);

for c = 1:length(P)-1

    x(c) = (TR+SL(c)*P(c))/(SL(c)-F);
    y(c) = F*x(c)+TR;
    X_P = [P(c) x(c)];
    Y_P = [0 y(c)];
    plot(X_P,Y_P,'r');

end

hold on

%%
 TM = T_max*DTOR;
 xw(1) = (TR+SL(1)*P(1))/(SL(1)-tan(TM));
 yw(1) = tan(TM)*xw(1)+TR;
 X_P2 = [P(1) xw];
 Y_P2 = [P(2) yw];
 plot(X_P2,Y_P2,'r');)
 DTW = tan(TM)/(length(P)-1);
 s(1) = tan(TM);
 b(1) = TR;

   for k = 2:length(P)-1

        s(k) = tan(TM)-(k-1)*DTW;
        b(k) = yw(k-1)-s(k)*xw(k-1);
        xw(k) = (b(k)+SL(k)*P(k))/(SL(k)-s(k));
        yw(k) = s(k)*xw(k)+b(k);
        X_P3 = [x(k) xw(k)];
        Y_P3 = [y(k) yw(k)];
        plot(X_P3,Y_P3,'r');

    end

    hold on

    %Ultimo ponto
```

```
    xf = (b(length(b))+SL(length(SL))*P(length(P)))/SL(length(SL));
    yf = b(length(b));
    X_F = [P(length(P)) xf];
    Y_F = [0 yf];
    plot(X_F,Y_F,'r');

    xw = [0 xw];
    yw = [TR yw];

%% Temperature distribution

To = T_1;
Temp = [];
TTo = [];
St = length(M);

for i = 2:St

    TTo(i) = (1+((g-1)/2)*(M(i))^2)^(-1);

end

%TTo(St+1) = (1+((g-1)/2)*(Msub(St+1))^2)^(-1);

for i = 2:St

    Temp(i) = To*(1+((g-1)/2)*(M(i))^2)^(-1);

end

%Temp(St+1) = To*(1+((g-1)/2)*(Msub(St+1))^2)^(-1);

%% Velocity distribution

V = [];
%V(1) = v_t;

for i = 2:St

    V(i) = M(i)*sqrt(g*R*Temp(i));

end

%V(St+1) = Msub(St+1)*sqrt(g*R*T(St+1));

%% Density distribution
```

```
rho = [];
rhorhoo = [];
%rho(1) = p_t/(R*TT);

for i = 2:St

    rhorhoo(i) = (1+((g-1)/2)*(M(i))^2)^((-1)/(g-1));

end

for i = 2:St-1

    Area(i) = (pi*(yw(i)*0.001)^2);
    rho(i) = m_dot/(V(i)*Area(i));

end

%% Pressure distribution

Ps = [];
PPo = [];
%Ps(1) = p_t;

for i = 2:St

    PPo(i) = (1+((g-1)/2)*(M(i))^2)^((-g)/(g-1));

end

for i = 2:St-1

    Ps(i) = rho(i)*R*Temp(i);

end

xlswrite('NozzleExcel.xlsx',transpose(xw),'Divergent','A1:A62');
xlswrite('NozzleExcel.xlsx',transpose(yw),'Divergent','B1:B62');
xlswrite('NozzleExcel.xlsx',transpose(TTo),'Divergent','C1:C62');
xlswrite('NozzleExcel.xlsx',transpose(Temp),'Divergent','D1:D62');
xlswrite('NozzleExcel.xlsx',transpose(V),'Divergent','E1:E62');
xlswrite('NozzleExcel.xlsx',transpose(rhorhoo),'Divergent','F1:F62');
xlswrite('NozzleExcel.xlsx',transpose(Area),'Divergent','G1:G62');
xlswrite('NozzleExcel.xlsx',transpose(rho),'Divergent','H1:H62');
xlswrite('NozzleExcel.xlsx',transpose(PPo),'Divergent','I1:I62');
xlswrite('NozzleExcel.xlsx',transpose(Ps),'Divergent','J1:J62');

%% Plots
```

```
figure(6)

plot(M,'r')
grid on
xlabel('Station')
ylabel('Mach Number')
title('Distribution of the Mach Number
along the Divergent Section')

%%
figure(7)
subplot(2,1,1)
plot(Temp,'r')
grid on
xlabel('Station')
ylabel('Static Temperature [K]')
title('Distribution of the Static
Temperature along the Divergent Section')

subplot(2,1,2)
plot(TTo,'r')
grid on
xlabel('Station')
ylabel('Static to Total Temperature ratio')
title('Distribution of the Static to Total
Temperature ratio along the Divergent Section')

%%
figure(8)
subplot(2,1,1)
plot(rho,'r')
grid on
xlabel('Station')
ylabel('Static density [Kg/m^3]')
title('Distribution of the Static density along the Divergent Section')

subplot(2,1,2)
plot(rhorhoo,'r')
grid on
xlabel('Station')
ylabel('Static to Total density ratio')
title('Distribution of the Static to Total
density ratio along the Divergent Section')

%%
figure(9)
```

```
subplot(2,1,1)
plot(Ps,'r')
grid on
xlabel('Station')
ylabel('Static Pressure [Pa]')
title('Distribution of the Static Pressure along the Divergent Section')

subplot(2,1,2)
plot(PPo,'r')
grid on
xlabel('Station')
ylabel('Static to Total Pressure ratio')
title('Distribution of the Static to
Total Pressure ratio along the Divergent Section')

end
```

C Convergent Section Contour and Parameters

C.1 Case 1 - Mass Flow = 80 kg/s

Table 1: Case 1 - Convergent Section Parameters

r	x	A	A ratio	M	T	T/To	u	ρ/ρ_0	ρ	p/p_0	p
0.135	0.000	0.057	2.272	0.266	744.493	0.986	145.303	0.966	9.579	0.952	2047031
0.132	0.017	0.055	2.164	0.280	743.327	0.985	153.148	0.962	9.541	0.947	2035839
0.129	0.033	0.052	2.059	0.296	741.986	0.983	161.710	0.957	9.498	0.941	2023007
0.126	0.050	0.049	1.956	0.314	740.432	0.981	171.093	0.952	9.449	0.934	2008217
0.122	0.067	0.047	1.856	0.333	738.619	0.978	181.424	0.947	9.391	0.926	1991064
0.119	0.084	0.044	1.759	0.355	736.489	0.975	192.862	0.940	9.323	0.917	1971034
0.116	0.100	0.042	1.664	0.379	733.960	0.972	205.611	0.932	9.244	0.906	1947455
0.113	0.117	0.040	1.572	0.406	730.927	0.968	219.934	0.922	9.148	0.893	1919428
0.109	0.134	0.037	1.482	0.437	727.236	0.963	236.193	0.911	9.033	0.877	1885721
0.106	0.151	0.035	1.395	0.473	722.666	0.957	254.893	0.896	8.892	0.858	1844567
0.103	0.167	0.033	1.311	0.516	716.869	0.949	276.801	0.878	8.715	0.834	1793297
0.099	0.184	0.031	1.229	0.568	709.256	0.939	303.175	0.855	8.485	0.804	1727523
0.096	0.201	0.029	1.150	0.635	698.675	0.925	336.416	0.824	8.172	0.762	1638993
0.093	0.217	0.027	1.074	0.731	682.165	0.904	382.558	0.776	7.698	0.701	1507392
0.090	0.234	–	–	–	–	–	–	–	–	–	–

C.2 Case 2 - Mass Flow = 60 kg/s

Table 2: Case 2 - Convergent Section Parameters

r	x	A	A ratio	M	T	T/To	u	ρ/ρ_0	ρ	p/p_0	p
0.117	0.000	0.043	2.272	0.266	744.493	0.986	145.303	0.966	9.579	0.952	2047031
0.114	0.014	0.041	2.164	0.280	743.327	0.985	153.148	0.962	9.541	0.947	2035839
0.112	0.029	0.039	2.059	0.296	741.986	0.983	161.710	0.957	9.498	0.941	2023007
0.109	0.043	0.037	1.956	0.314	740.432	0.981	171.093	0.952	9.449	0.934	2008217
0.106	0.058	0.035	1.856	0.333	738.619	0.978	181.424	0.947	9.391	0.926	1991064
0.103	0.072	0.033	1.759	0.355	736.489	0.975	192.862	0.940	9.323	0.917	1971034
0.100	0.087	0.032	1.664	0.379	733.960	0.972	205.611	0.932	9.244	0.906	1947455
0.097	0.101	0.030	1.572	0.406	730.927	0.968	219.934	0.922	9.148	0.893	1919428
0.095	0.116	0.028	1.482	0.437	727.236	0.963	236.193	0.911	9.033	0.877	1885721
0.092	0.130	0.026	1.395	0.473	722.666	0.957	254.893	0.896	8.892	0.858	1844567
0.089	0.145	0.025	1.311	0.516	716.869	0.949	276.801	0.878	8.715	0.834	1793297
0.086	0.159	0.023	1.229	0.568	709.256	0.939	303.175	0.855	8.485	0.804	1727523
0.083	0.174	0.022	1.150	0.635	698.675	0.925	336.416	0.824	8.172	0.762	1638993
0.081	0.188	0.020	1.074	0.731	682.165	0.904	382.558	0.776	7.698	0.701	1507392
0.078	0.203	–	–	–	–	–	–	–	–	–	–

C.3 Case 3 - Mass Flow = 40 kg/s

Table 3: Case 3 - Convergent Section Parameters

r	x	A	A ratio	M	T	T/To	u	ρ/ρ_0	ρ	p/p_0	p
0.096	0.000	0.029	2.272	0.266	744.493	0.986	145.303	0.966	9.579	0.952	2047031
0.093	0.012	0.027	2.164	0.280	743.327	0.985	153.148	0.962	9.541	0.947	2035839
0.091	0.024	0.026	2.059	0.296	741.986	0.983	161.710	0.957	9.498	0.941	2023007
0.089	0.035	0.025	1.956	0.314	740.432	0.981	171.093	0.952	9.449	0.934	2008217
0.086	0.047	0.023	1.856	0.333	738.619	0.978	181.424	0.947	9.391	0.926	1991064
0.084	0.059	0.022	1.759	0.355	736.489	0.975	192.862	0.940	9.323	0.917	1971034
0.082	0.071	0.021	1.664	0.379	733.960	0.972	205.611	0.932	9.244	0.906	1947455
0.080	0.083	0.020	1.572	0.406	730.927	0.968	219.934	0.922	9.148	0.893	1919428
0.077	0.095	0.019	1.482	0.437	727.236	0.963	236.193	0.911	9.033	0.877	1885721
0.075	0.106	0.018	1.395	0.473	722.666	0.957	254.893	0.896	8.892	0.858	1844567
0.073	0.118	0.017	1.311	0.516	716.869	0.949	276.801	0.878	8.715	0.834	1793297
0.070	0.130	0.016	1.229	0.568	709.256	0.939	303.175	0.855	8.485	0.804	1727523
0.068	0.142	0.015	1.150	0.635	698.675	0.925	336.416	0.824	8.172	0.762	1638993
0.066	0.154	0.014	1.074	0.731	682.165	0.904	382.558	0.776	7.698	0.701	1507392
0.063	0.166	–	–	–	–	–	–	–	–	–	–

D Divergent Section Contour and Parameters

D.1 Case 1 - Mass Flow = 80 kg/s

Table 4: Case 1 - Divergent Section Parameters

$x(mm)$	$r(mm)$	T/To	T	u	ρ/ρ_0	A	ρ	p/p_0	p
0.000	89.700	0.000	0.000	0.000	0.000	0.000	0.000	0.000	0
5.157	91.823	0.801	604.713	549.526	0.574	0.026	5.496	0.460	954021
8.389	93.122	0.788	594.711	567.519	0.551	0.027	5.174	0.434	883317
11.671	94.410	0.776	585.568	583.480	0.530	0.028	4.896	0.411	823018
15.005	95.687	0.764	576.940	598.152	0.510	0.029	4.650	0.390	770040
18.391	96.951	0.753	568.660	611.900	0.492	0.030	4.427	0.371	722713
21.832	98.202	0.743	560.634	624.940	0.475	0.030	4.225	0.353	679976
25.329	99.441	0.732	552.800	637.410	0.459	0.031	4.040	0.336	641086
28.883	100.666	0.722	545.117	649.406	0.443	0.032	3.870	0.320	605491
32.497	101.876	0.712	537.557	660.998	0.428	0.033	3.712	0.305	572762
36.172	103.072	0.702	530.099	672.239	0.413	0.033	3.566	0.290	542556
39.909	104.253	0.692	522.725	683.170	0.399	0.034	3.430	0.276	514592
43.712	105.418	0.683	515.425	693.823	0.385	0.035	3.303	0.263	488635
47.581	106.566	0.673	508.187	704.226	0.372	0.036	3.184	0.250	464484
51.519	107.697	0.664	501.005	714.398	0.359	0.036	3.073	0.238	441970
55.527	108.810	0.654	493.872	724.360	0.346	0.037	2.969	0.226	420943
59.608	109.903	0.645	486.784	734.125	0.334	0.038	2.872	0.215	401274
63.764	110.978	0.635	479.736	743.708	0.322	0.039	2.780	0.205	382849
67.997	112.031	0.626	472.726	753.118	0.310	0.039	2.694	0.194	365566
72.310	113.063	0.617	465.751	762.367	0.299	0.040	2.613	0.184	349337
76.704	114.073	0.608	458.808	771.462	0.288	0.041	2.537	0.175	334080
81.183	115.059	0.599	451.896	780.411	0.277	0.042	2.465	0.166	319723
85.748	116.020	0.589	445.015	789.220	0.267	0.042	2.397	0.157	306200
90.403	116.956	0.580	438.162	797.896	0.257	0.043	2.333	0.149	293454
95.150	117.865	0.571	431.337	806.444	0.247	0.044	2.273	0.141	281431
99.993	118.745	0.562	424.541	814.867	0.237	0.044	2.216	0.133	270082
104.933	119.597	0.553	417.771	823.171	0.228	0.045	2.163	0.126	259362
109.974	120.417	0.544	411.029	831.359	0.219	0.046	2.112	0.119	249232
115.120	121.205	0.536	404.314	839.435	0.210	0.046	2.065	0.112	239655
120.373	121.959	0.527	397.626	847.401	0.201	0.047	2.020	0.106	230596
125.737	122.678	0.518	390.966	855.261	0.193	0.047	1.978	0.100	222025
131.216	123.360	0.509	384.334	863.017	0.185	0.048	1.939	0.094	213913
136.812	124.003	0.500	377.730	870.670	0.177	0.048	1.902	0.089	206234
142.531	124.605	0.492	371.155	878.225	0.169	0.049	1.868	0.083	198964
148.376	125.165	0.483	364.609	885.682	0.162	0.049	1.835	0.078	192080
154.352	125.679	0.474	358.093	893.043	0.155	0.050	1.805	0.073	185563
160.462	126.147	0.466	351.607	900.309	0.148	0.050	1.777	0.069	179393
166.712	126.566	0.457	345.153	907.483	0.141	0.050	1.752	0.065	173554
173.105	126.933	0.449	338.731	914.566	0.135	0.051	1.728	0.060	168029
179.648	127.246	0.440	332.341	921.559	0.129	0.051	1.707	0.057	162804
186.345	127.503	0.432	325.984	928.463	0.122	0.051	1.687	0.053	157866
193.202	127.700	0.423	319.662	935.279	0.117	0.051	1.670	0.049	153202
200.225	127.834	0.415	313.375	942.008	0.111	0.051	1.654	0.046	148803
207.419	127.903	0.407	307.124	948.652	0.106	0.051	1.641	0.043	144657
–	–	0.399	300.910	955.210	0.100	–	–	0.040	–

D.2 Case 2 - Mass Flow = 60 kg/s

Table 5: Case 2 - Divergent Section Parameters

$x(mm)$	$r(mm)$	T/To	T	u	ρ/ρ_0	A	ρ	p/p_0	p
0.000	77.700	0.000	0.000	0.000	0.000	0.000	0.000	0.000	0
4.467	79.539	0.801	604.713	549.526	0.574	0.020	5.494	0.460	953591
7.267	80.664	0.788	594.711	567.519	0.551	0.020	5.172	0.434	882919
10.110	81.780	0.776	585.568	583.480	0.530	0.021	4.894	0.411	822647
12.998	82.886	0.764	576.940	598.152	0.510	0.022	4.648	0.390	769693
15.931	83.981	0.753	568.660	611.900	0.492	0.022	4.425	0.371	722387
18.911	85.065	0.743	560.634	624.940	0.475	0.023	4.223	0.353	679669
21.940	86.138	0.732	552.800	637.410	0.459	0.023	4.038	0.336	640797
25.019	87.199	0.722	545.117	649.406	0.443	0.024	3.868	0.320	605218
28.149	88.248	0.712	537.557	660.998	0.428	0.024	3.710	0.305	572504
31.333	89.284	0.702	530.099	672.239	0.413	0.025	3.564	0.290	542312
34.570	90.306	0.692	522.725	683.170	0.399	0.026	3.428	0.276	514360
37.864	91.315	0.683	515.425	693.823	0.385	0.026	3.301	0.263	488414
41.216	92.310	0.673	508.187	704.226	0.372	0.027	3.183	0.250	464275
44.626	93.289	0.664	501.005	714.398	0.359	0.027	3.072	0.238	441770
48.099	94.253	0.654	493.872	724.360	0.346	0.028	2.968	0.226	420753
51.634	95.201	0.645	486.784	734.125	0.334	0.028	2.870	0.215	401093
55.234	96.131	0.635	479.736	743.708	0.322	0.029	2.779	0.205	382676
58.901	97.044	0.626	472.726	753.118	0.310	0.030	2.693	0.194	365401
62.636	97.938	0.617	465.751	762.367	0.299	0.030	2.612	0.184	349179
66.443	98.812	0.608	458.808	771.462	0.288	0.031	2.536	0.175	333929
70.322	99.666	0.599	451.896	780.411	0.277	0.031	2.464	0.166	319578
74.277	100.499	0.589	445.015	789.220	0.267	0.032	2.396	0.157	306062
78.309	101.310	0.580	438.162	797.896	0.257	0.032	2.332	0.149	293322
82.421	102.097	0.571	431.337	806.444	0.247	0.033	2.272	0.141	281304
86.616	102.860	0.562	424.541	814.867	0.237	0.033	2.215	0.133	269960
90.895	103.597	0.553	417.771	823.171	0.228	0.034	2.162	0.126	259245
95.262	104.308	0.544	411.029	831.359	0.219	0.034	2.111	0.119	249120
99.719	104.990	0.536	404.314	839.435	0.210	0.035	2.064	0.112	239547
104.269	105.644	0.527	397.626	847.401	0.201	0.035	2.019	0.106	230492
108.916	106.266	0.518	390.966	855.261	0.193	0.035	1.977	0.100	221925
113.662	106.857	0.509	384.334	863.017	0.185	0.036	1.938	0.094	213817
118.510	107.414	0.500	377.730	870.670	0.177	0.036	1.901	0.089	206141
123.464	107.936	0.492	371.155	878.225	0.169	0.037	1.867	0.083	198874
128.527	108.420	0.483	364.609	885.682	0.162	0.037	1.834	0.078	191994
133.703	108.866	0.474	358.093	893.043	0.155	0.037	1.804	0.073	185479
138.996	109.271	0.466	351.607	900.309	0.148	0.038	1.777	0.069	179313
144.409	109.634	0.457	345.153	907.483	0.141	0.038	1.751	0.065	173476
149.947	109.952	0.449	338.731	914.566	0.135	0.038	1.727	0.060	167953
155.615	110.224	0.440	332.341	921.559	0.129	0.038	1.706	0.057	162731
161.416	110.446	0.432	325.984	928.463	0.122	0.038	1.686	0.053	157795
167.356	110.616	0.423	319.662	935.279	0.117	0.038	1.669	0.049	153133
173.439	110.733	0.415	313.375	942.008	0.111	0.039	1.653	0.046	148736
179.670	110.792	0.407	307.124	948.652	0.106	0.039	1.640	0.043	144592
–	–	0.399	300.910	955.210	0.100	–	–	0.040	–

D.3 Case 3 - Mass Flow = 40 kg/s

Table 6: Case 3 - Divergent Section Parameters

$x(mm)$	$r(mm)$	T/To	T	u	ρ/ρ_0	A	ρ	p/p_0	p
0.000	63.500	0.000	0.000	0.000	0.000	0.000	0.000	0.000	0
3.651	65.003	0.801	604.713	549.526	0.574	0.013	5.484	0.460	951843
5.939	65.923	0.788	594.711	567.519	0.551	0.014	5.163	0.434	881301
8.262	66.835	0.776	585.568	583.480	0.530	0.014	4.885	0.411	821139
10.622	67.738	0.764	576.940	598.152	0.510	0.014	4.639	0.390	768282
13.019	68.633	0.753	568.660	611.900	0.492	0.015	4.417	0.371	721063
15.455	69.519	0.743	560.634	624.940	0.475	0.015	4.216	0.353	678424
17.930	70.396	0.732	552.800	637.410	0.459	0.016	4.031	0.336	639622
20.447	71.263	0.722	545.117	649.406	0.443	0.016	3.861	0.320	604108
23.005	72.120	0.712	537.557	660.998	0.428	0.016	3.703	0.305	571454
25.606	72.967	0.702	530.099	672.239	0.413	0.017	3.557	0.290	541318
28.252	73.802	0.692	522.725	683.170	0.399	0.017	3.422	0.276	513417
30.944	74.627	0.683	515.425	693.823	0.385	0.017	3.295	0.263	487519
33.683	75.440	0.673	508.187	704.226	0.372	0.018	3.177	0.250	463424
36.471	76.240	0.664	501.005	714.398	0.359	0.018	3.066	0.238	440961
39.308	77.028	0.654	493.872	724.360	0.346	0.019	2.963	0.226	419982
42.197	77.802	0.645	486.784	734.125	0.334	0.019	2.865	0.215	400358
45.140	78.563	0.635	479.736	743.708	0.322	0.019	2.774	0.205	381975
48.136	79.309	0.626	472.726	753.118	0.310	0.020	2.688	0.194	364732
51.189	80.039	0.617	465.751	762.367	0.299	0.020	2.607	0.184	348539
54.300	80.754	0.608	458.808	771.462	0.288	0.020	2.531	0.175	333317
57.470	81.452	0.599	451.896	780.411	0.277	0.021	2.459	0.166	318993
60.702	82.132	0.589	445.015	789.220	0.267	0.021	2.392	0.157	305501
63.998	82.795	0.580	438.162	797.896	0.257	0.022	2.328	0.149	292784
67.358	83.438	0.571	431.337	806.444	0.247	0.022	2.268	0.141	280788
70.786	84.062	0.562	424.541	814.867	0.237	0.022	2.211	0.133	269465
74.284	84.664	0.553	417.771	823.171	0.228	0.023	2.158	0.126	258770
77.852	85.245	0.544	411.029	831.359	0.219	0.023	2.108	0.119	248663
81.495	85.803	0.536	404.314	839.435	0.210	0.023	2.060	0.112	239108
85.214	86.337	0.527	397.626	847.401	0.201	0.023	2.016	0.106	230070
89.011	86.846	0.518	390.966	855.261	0.193	0.024	1.974	0.100	221518
92.889	87.328	0.509	384.334	863.017	0.185	0.024	1.935	0.094	213425
96.852	87.784	0.500	377.730	870.670	0.177	0.024	1.898	0.089	205763
100.900	88.210	0.492	371.155	878.225	0.169	0.024	1.863	0.083	198510
105.038	88.606	0.483	364.609	885.682	0.162	0.025	1.831	0.078	191642
109.268	88.970	0.474	358.093	893.043	0.155	0.025	1.801	0.073	185140
113.594	89.302	0.466	351.607	900.309	0.148	0.025	1.773	0.069	178984
118.018	89.598	0.457	345.153	907.483	0.141	0.025	1.748	0.065	173158
122.544	89.858	0.449	338.731	914.566	0.135	0.025	1.724	0.060	167645
127.176	90.080	0.440	332.341	921.559	0.129	0.025	1.703	0.057	162432
131.917	90.261	0.432	325.984	928.463	0.122	0.026	1.683	0.053	157506
136.771	90.401	0.423	319.662	935.279	0.117	0.026	1.666	0.049	152853
141.742	90.496	0.415	313.375	942.008	0.111	0.026	1.650	0.046	148463
146.835	90.545	0.407	307.124	948.652	0.106	0.026	1.637	0.043	144327
–	–	0.399	300.910	955.210	0.100	–	–	0.040	–

E Properties of the Earth's Standard Atmosphere

Table 7: International Standard Atmosphere Properties [9].

Sea-level pressure is 0.101325 MPa (or 14.696 psia or 1.000 atm).

Altitude (m)	Temperature (K)	Pressure Ratio	Density (kg/m^3)
0 (sea level)	288.150	1.0000	1.2250
1,000	281.651	8.8700×10^{-1}	1.1117
3,000	268.650	6.6919×10^{-1}	9.0912×10^{-1}
5,000	255.650	5.3313×10^{-1}	7.6312×10^{-1}
10,000	223.252	2.6151×10^{-1}	4.1351×10^{-1}
25,000	221.552	2.5158×10^{-2}	4.0084×10^{-2}
50,000	270.650	7.8735×10^{-4}	1.0269×10^{-3}
75,000	206.650	2.0408×10^{-5}	3.4861×10^{-5}
100,000	195.08	3.1593×10^{-7}	5.604×10^{-7}
130,000	469.27	1.2341×10^{-8}	8.152×10^{-9}
160,000	696.29	2.9997×10^{-9}	1.233×10^{-9}
200,000	845.56	8.3628×10^{-10}	2.541×10^{-10}
300,000	976.01	8.6557×10^{-11}	1.916×10^{-11}
400,000	995.83	1.4328×10^{-11}	2.803×10^{-12}
600,000	999.85	8.1056×10^{-13}	2.137×10^{-13}
1,000,000	1000.00	7.4155×10^{-14}	3.561×10^{-15}